

Drug research program
Division of pharmaceutical Biosciences
Faculty of Pharmacy
Doctoral programme in drug research
University of Helsinki
Finland

THE USE OF MOLECULAR DYNAMICS SIMULATION FOR THE STUDY OF POLYMERIC AND LIPID BASED DRUG DELIVERY SYSTEMS

Mohammad Mahmoudzadeh

ACADEMIC DISSERTATION

Doctoral thesis to be presented for public examination with the permission of the Faculty of Pharmacy of the University of Helsinki, in Auditorium 1041, Biocenter 2, Viikinkaari 5, on the 11th of November 2022 at 13 o'clock.

Helsinki 2022

Supervisors: Docent Alex Bunker
Division of Pharmaceutical Biosciences
Faculty of Pharmacy
University of Helsinki
Finland

Dr. Artturi Koivuniemi
Division of Pharmaceutical Biosciences
Faculty of Pharmacy
University of Helsinki
Finland

Pre-examiners: Professor Prabal Maiti
Center for Condensed Matter Theory,
Department of Physics,
Indian Institute of Science
Bangalore, India

Associate Professor Per Larsson
Department of Pharmacy, drug delivery
Uppsala University
Uppsala, Sweden

Opponent: Associate Professor Defang Ouyang
Institute of Chinese Medical Sciences (ICMS)
University of Macau, Macau, China

© Mohammad Mahmoudzadeh

ISBN 978-951-51-8672-0 (print)
ISBN 978-951-51-8673-7 (online)

Published in Doctoral School of Health series *Dissertationes Scholae Doctoralis Ad Sanitatem Investigandam Universitatis Helsinkiensis* 64/2022.

ISSN 2342-3161 (print)
ISSN 2342-317X (online)

The Faculty of Pharmacy uses the Ouriginal system (plagiarism recognition) to examine all doctoral dissertations.

Unigrafia, Helsinki, Finland, 2022

ABSTRACT

Systemic administration is the conventional method for administering drugs. Following injection, ideally, we wish the drug only to locate to the target tissue, however, this is not what occurs; the drug molecules rather distribute throughout the entire body via the blood stream. Regarding some drugs, in particular chemotherapy agents, this often leads to severe dose limiting side effects and unsatisfactory therapeutic results. On the other hand, many drugs as is also the case for the chemotherapy agents, demonstrate low aqueous solubility and suboptimal pharmacokinetic properties. These problems all necessitate the use of drug delivery systems (DDSs) as they decrease the side effects of drugs while also improving drug bioavailability and pharmacokinetics.

Although there are different varieties of DDSs, we have focused on those categorized as polymeric or lipidic. Depending on the drug to be delivered and site of action of the drug, polymeric DDSs can be used either locally or systemically. Hydrogels and electrospun polymer fibers are two examples of polymeric DDSs that are used for the local delivery of many drugs, including antibiotics and anticancer drugs.

The other form of polymeric DDSs are nanoparticles that are capable of carrying and in some cases targeting drug molecules. These polymeric DDSs are generally injected into the blood stream to reach their target site.

Lipidic DDSs mainly are used in the form of nanoparticles that, depending on their lipid composition and method of preparation, would have different characteristics. Liposomes and solid lipid nanoparticles are two examples of lipidic DDSs.

Despite the huge number of publications regarding the use of nanoparticles as DDSs, the number of approved drug therapies that make use of nanoparticle-based delivery systems still remains small. One of the reasons for this problem is that formulations of DDSs are complicated and difficult to optimize. Drug delivery systems should be further redesigned and optimized, however, this has proved challenging due to intrinsic and practical

experimental limitations. For example, it is difficult to experimentally elucidate the reason many DDSs show promise in vitro but fail in vivo. The limitations to the extent to which mechanistic insight can be gained from experiments regarding DDSs can be compensated by computational molecular modelling techniques that provide detailed information on molecular interactions of drugs and carriers. The insights obtained by the studies performed in this thesis can be used to improve the design of DDSs.

In this thesis, two polymeric (studies **I and IV**) and two lipidic (studies **II and III**) DDSs were studied by all-atom molecular dynamics (MD) simulations. In each of these studies, a specific property of the DDS was evaluated in detail. These properties are drug release profile (study **I**), stability (study **II**), pH-sensitivity (study **III**) and size (study **IV**). We evaluated these properties through investigation of the three varieties of interactions DDSs have: interactions of DDSs with the loaded drug, interactions among the components of DDSs and interactions between the DDSs and the medium, namely water and ions. While it is difficult to directly determine an accurate picture of these interactions experimentally at atomic scale resolution, all-atom MD simulation can provide insight into this.

ACKNOWLEDGEMENTS

The work presented in this thesis was carried out in the Division of Pharmaceutical Biosciences, Faculty of Pharmacy, University of Helsinki during the years 2016-2022. I owe completing my doctoral education to my supervisors, family, friends and the foundations who financially supported me.

I would like to thank my supervisors Doc. Alex Bunker and Dr. Artturi Koivuniemi. I am grateful to Doc. Alex Bunker for providing me the chance to start and continue my doctoral education in the Faculty of Pharmacy, University of Helsinki. I appreciate the scientific support of Dr. Artturi Koivuniemi during my doctoral education. His supportive and professional attitude as a supervisor has had a big role in my success to complete my doctoral thesis.

I would also like to express my gratitude to all my friends with whom spending time, provided me with energy to work better. I thank Dr. Amir Sadeghi for her valuable friendship during the last twenty years, a friend with whom I made the fundamentals of my academic carrier. I would like to thank Dr. Kourosch Kabiri for his valuable friendship with me since the time I came to Finland. I would like to thank Ali Ashrafzadeh, Yahya, Ali Tavakoli, Bahram, Iman, Manlio, Cristina, Polina, Heidi, Tuomas and Pia.

I wish to thank my mother, brother and sister who always were a source of energy for me to go forward. I dedicate my doctoral thesis to the soul of my father who always encouraged me to learn new things and not to be afraid of the difficulties. My special thanks goes to my wife without her patience, strength and kindness, I would not manage to complete my doctoral education.

I would like to thank the grants from the Center for international mobility, Academy of Finland, Magnus Ehrnrooth Foundation, ÖLVI foundation, Tor, Joe and Pentti Borg foundation, Finnish-Norwegian Medical Foundation, Lasten syöpäsäätiö Väre, Ida Montin Foundation and Waldemar Von Frenckell Foundation. I would also like to acknowledge the computational resources of the Finnish IT Centre for Scientific Computing (CSC).

Mohammad Mahmoudzadeh October 2022, Helsinki

CONTENTS

1	Introduction.....	1
2	Review of the literature	5
2.1	polymeric drug delivery systems	5
2.1.1	Local polymeric drug delivery systems	5
2.1.1.1	Electrospun fibers	5
2.1.1.2	Hydrogels	7
2.1.2	Polymeric nanoparticles.....	11
2.2	Lipidic drug delivery systems.....	15
2.2.1	PEGylated liposomes.....	17
2.2.2	pH-sensitive liposomes.....	21
3	Aims of the study.....	25
4	Overview of the methods.....	27
4.1	Computational modelling of drug delivery systems.....	27
4.2	Molecular dynamics simulations.....	28
4.2.1	Periodic boundary conditions.....	29
4.2.2	Different stages of MD simulations.....	29
4.2.3	Ensembles, thermostats and barostates in MD simulations.....	31
4.2.4	Force fields.....	34
4.2.4.1	Bonded interactions.....	36
4.2.4.2	non-bonded interactions.....	37
4.2.5	Calculating non-bonded interactions.....	40

4.2.6	Limitations of all-atom MD simulation for the study of DDSs.....	41
5	Results and discussion.....	43
5.1	Drug release.....	43
5.2	Stability.....	46
5.3	pH-sensitivity.....	48
5.4	Size.....	51
6	Conclusions	55
7	References.....	57

LIST OF ORIGINAL PUBLICATIONS

This thesis is based on the following studies:

I Liis Preem, **Mohammad Mahmoudzadeh**, Marta Putrinš, Andres Meos, Ivo Laidmäe, Tavo Romann, Jaan Aruväli, Riinu Härmäs, Artturi Koivuniemi, Alex Bunker, Tanel Tenson, Karin Kogermann; Interactions between Chloramphenicol, Carrier Polymers, and Bacteria– Implications for Designing Electrospun Drug Delivery Systems Countering Wound Infection, **Molecular Pharmaceutics**, 2017; **14 (12): 4417-4430**.

II Francesca Mastrotto, Chiara Brazzale, Federica Bellato, Sara De Martin, Guillaume Grange, **Mohamad Mahmoudzadeh**, Aniket Magarkar, Alex Bunker, Stefano Salmaso, Paolo Caliceti; In vitro and in vivo behavior of liposomes decorated with PEGs with different chemical features, **Molecular Pharmaceutics**, 2020; **17 (2): 472-487**. *

III **Mohammad Mahmoudzadeh**, Aniket Magarkar, Artturi Koivuniemi, Tomasz Róg, Alex Bunker; Mechanistic Insight into How PEGylation Reduces the Efficacy of pH-Sensitive Liposomes from Molecular Dynamics Simulations, **Molecular Pharmaceutics**, 2021; **18 (7) :2612-2621**.

IV Zehua Liu, Wenhua Lian, Qiang Long, Ruoyu Cheng, Giulia Torrieri, Baoding Zhang, Artturi Koivuniemi, **Mohammad Mahmoudzadeh**, Alex Bunker, Han Gao, Hongbin He, Yun Chen , Jouni Hirvonen, Rongbin Zhou, Qiang Zhao, Xiaofeng Ye, Xianming Deng, Hélder A. Santos; Promoting cardiac repair through simple engineering of nanoparticles with exclusive targeting capability towards myocardial reperfusion injury by thermal resistant microfluidic platform; **Advanced functional materials**, 2022; **32 (36), 2204666**.

The studies conducted in this thesis are referred to in the text by their roman numerals.

* This article has been corrected. Correction can be found in *Mol. Pharmaceutics* 2020, 17, 4, 1444. The correction is that on page 472 of the paper and on page 1 of the supporting information, the name of the coauthor Mohamad Mahmoudzadeh is spelled incorrectly. The correct name of this coauthor is Mohammad Mahmoudzadeh.

AUTHOR CONTRIBUTION

Study I

The author (M.M) contributed to the study design of the computational section, built the computational models, conducted quantum calculations, performed docking studies and molecular dynamics simulations and performed the analysis and extracted the results of the computational section. He contributed to writing the computational section in the first draft of the manuscript.

Study II

The author (M.M) performed most of the analysis and extracted most of the results of the computational section. The author contributed to writing the computational section in the first draft of the manuscript.

Study III

The author (M.M) conducted some of the molecular dynamics simulations, performed the analysis and extracted the results. The author wrote the first draft of the manuscript and revised it with the help of co-authors.

Study IV

The author (M.M) contributed to the study design of the section related to the molecular dynamics simulations, performed most of the analysis and extracted most of the results related to the molecular dynamics simulations. The author contributed to writing the section related to molecular dynamics simulations in the first draft of the manuscript.

ABBREVIATIONS

DDSs	Drug Delivery Systems
MD	Molecular Dynamics
CS	Chitosan
PEG	Poly Ethylene Glycol
PCL	Poly caprolactone
PLGA	Poly lactic-co-glycolic acid
CG	Coarse-grained
CIP	Ciprofloxacin
HP β CD	Hydroxypropyl-beta-cyclodextrin
PVA	Poly vinyl alcohol
PLA	Poly lactic acid
H-bond	Hydrogen bond
PCBMA	poly (carboxybetaine methacrylate)
OH-PCBMA	Hydroxylated poly(carboxybetaine methacrylate)
EPR	Enhanced permeability and retention effect
Poly(OEGA)	Poly(oligo(ethylene glycol) methyl ether acrylate)
PFPE	Perfluoropolyether
POPC	1-palmitoyl-2-oleoyl-sn-glycero-3-phosphocholine
DSPC	1,2-Distearoyl-sn-glycero-3-phosphocholine
DOPE	1,2-Dioleoyl-sn-glycero-3-phosphoethanolamine
MPS	Mononuclear Phagocytic System
PSPC	1-palmitoyl-2-stearoyl-sn-glycero-3-phosphocholine
DSPE	1,2-distearoyl-sn-glycero-3-phosphoethanolamine
HII	Inverted hexagonal
PE	Phosphatidylethanolamine
CHMS	Cholesteryl hemisuccinate
R _w	Radius of the water core
d _{hex}	lattice plane distance
CHSa	Deprotonated (anionic) form of Cholesteryl hemisuccinate
CHS	Protonated (neutral) form of Cholesteryl hemisuccinate
MC	Monte Carlo
HPC	High Performance Computing
MPI	Messaging Passing Interface
GPUs	Graphical Processing Units
LJ	Lennard-Jones
RESP	Restrained Electrostatic Potential
PME	Particle mesh Ewald
PEO	Polyethylene Oxide
CAM	Chloramphenicol
Chol	Cholesterol
Chln	Cholane

PG

Phosphorylated Glucan

1 INTRODUCTION

During the past decades, DDSs have gained significant research interest in the pharmaceutical industry especially for the purpose of the delivery of anticancer drugs [1-3]. Drug delivery systems improve the bioavailability and pharmacokinetics of anticancer drugs by accumulating drug in the target tissue and controlling the release of the drug. Systemic administration of anticancer drugs as the conventional method of administration of these drugs, often leads to severe dose limiting toxicity (Myelosuppression, neutropenia and leucopenia), unsatisfactory therapeutic results [4] and severe side effects, for example cardiac dysfunction and heart failure [5, 6].

On the other hand, most of the anti-cancer drugs, demonstrate low aqueous solubility due to their lipophilic structure that makes formulating them in aqueous solvents difficult. Therefore, they must be formulated in non-aqueous solvents, for example Paclitaxel in Taxol® is formulated in polyethoxylated castor oil (Cremophor EL) and Docetaxel in Taxotere®, is formulated in Tween 80 (a nonionic surfactant). For both of these non-aqueous solvents, severe hyper sensitivity reactions have been reported [7]. Dose limiting toxicity, severe side effects and difficulty in formulation of anti-cancer drugs have encouraged scientists to use DDSs for their delivery.

Depending on the drug to be delivered and site of action of the drug, DDSs are designed to be used either locally or systemically. Drug delivery systems that involve local application are generally three-dimensional polymeric networks cross-linked chemically or physically where the loaded drug is distributed within the polymeric network. Two examples of such systems are hydrogels [8, 9] and electrospun fibers [10, 11].

Drug delivery systems intended for systemic administration are generally formulated as nanoparticles; we have focused on the subset that are polymeric or lipidic. The polymeric DDSs are rapidly being developed using natural and synthetic polymers [12] as their building blocks and play an important role in different pharmaceutical fields. Chitosan (CS) [13] and dextran [14] are examples of natural polymers and Polyethylene glycol (PEG),

Polycaprolactone (PCL) and Poly lactic-co-glycolic acid (PLGA) [15] are examples of synthetic polymers used for drug delivery purposes. The drug to be delivered by polymeric DDSs would be entrapped, encapsulated or bound to polymeric NPs in the form of a nanosphere, nanocapsule or drug conjugate using different preparation methods [16]. Polymeric micelles and dendrimers are two examples of polymeric DDSs.

The most important lipid nanoparticles are liposomes. The main component of liposomes are phospholipids that self-assemble into lipid bilayers upon hydration. They are versatile carriers capable of loading hydrophilic drugs within their internal cavity or hydrophobic drugs within the liposome membrane. As such, they are a very promising DDS; liposome based DDSs have been FDA approved mainly for treatment of cancer and infections [17]. The composition of liposomes determines their physicochemical properties. Liposomes that are used for drug delivery purposes generally have a protective polymer coating to increase their blood circulation time. Polyethylene glycol is the most common polymer used for this purpose [18].

An ideal DDS has the five following characteristics: 1- biocompatible and biodegradable 2- high drug loading capacity 3- long blood circulation time 4- high accumulation in target tissue 5- controlled release profile. Optimizing these parameters can be performed to some extent experimentally, for example through changing the composition and the method used to prepare the nanoparticles. However, regarding performance and optimization of DDSs certain questions frequently arise that are difficult to address experimentally. In such cases MD simulation can be of help when it is necessary to know the specific interactions between different components of a drug loaded DDS and when mechanisms behind an experimental observation need to be elucidated. With two examples, I try to elaborate on occasions where MD simulation has the capacity to complement the experimental development and optimization of DDSs through providing insight that is difficult or impossible to be obtained experimentally.

Example 1: it is experimentally very difficult if not impossible to determine why Zhang et al. [19] observed that, with an increase in the degree of substitution of hydrophobic octyl groups on trimethyl Chitosan from 8% to

58%, the ability of loading the hydrophobic anticancer drug Hydroxy Camptothecin into polymeric micelles formed, decreased from 32.5% to 8.6%. This is while most of the other groups loading drugs into hydrophobically modified Chitosan polymeric micelles have reported an increase in drug loading capacity for hydrophobic drugs with increasing degree of substitution of the hydrophobic groups of the Chitosan polymer [20].

Example 2: Although size of the drug-loaded polymeric micelles generally increases as a result of an increase in the loaded drug amount, Lao et al. [21] observed that with loading Rotenone in N-(octadecanol-1-glycidyl ether)-O-sulfate chitosan micelles, the size of the micelles reduced from 180.7 to 116.4 nm. In justification of this unusual observation, they wrote in their article: “Probably there had been the hydrophobic interaction between chitosan derivative and rotenone”. Here is the place that MD simulation can be brought to bear and replace the word “probably” with a more robust answer.

Depending on the variety of interactions to be studied and the question we wish to answer regarding the characteristics and performance of a DDS, there exists two possible approaches for using MD simulations. If the interactions within the nanoparticle itself or the interactions occurring on the surface is to be evaluated, detailed data would be obtained through simulating a section of a DDS using atomistic MD simulations. As the computational power grows enormously, atomistic MD simulations can be used to study larger and more complex systems. However, if the whole nanoparticle is to be simulated, coarse-grained (CG) MD simulations provide us with a bigger picture at the expense of losing atomistic details.

2 REVIEW OF THE LITERATURE

In this section, I will review in detail the most important polymeric and lipidic drug delivery systems and through some examples, will elaborate on the use of MD simulations for the study of these DDSs.

2.1 POLYMERIC DRUG DELIVERY SYSTEMS

2.1.1 LOCAL POLYMERIC DRUG DELIVERY SYSTEMS

2.1.1.1 *Electrospun fibers*

The most frequent method used to produce nano fibers for drug delivery purposes is Electrospinning [22-24] where fiber production is performed through stretching fibers from a viscoelastic polymer solution through electrostatic force. Electrospun polymer nanofibers have unique properties such as large surface area (the surface area of nanofibers with ~100 nm diameter is ~1000 m²/g [25]), high porosity with small pore sizes, strengthened mechanical properties and flexibility to be formulated in various shapes that makes them a promising DDS for local administration [26]. Due to these properties, electrospun polymer nanofibers have been used for the delivery of many drugs including Mefoxen, Ketoprofen, Naproxen, Indomethacin, Ibuprofen [27], cefazolin [28], acyclovir [29], Metronidazole [30] doxycycline [31] and 5-Fluorouracil [32].

One of the most important requirements for electrospun fibers to enter clinical applications is an appropriate drug release profile [33] that so far has not been obtained due to release problems such as incomplete drug release and the initial burst release. Due to high surface area, the initial burst release of the drug is a common characteristic of drug loaded electrospun fiber formulations [25]. To obtain electrospun nanofiber mats with the desired drug release properties, the composition of the polymers is very important [23, 25]. For example, when the drug to be loaded is hydrophobic, Zeng et al. [34]

recommended a lipophilic polymer to be used for the production of electrospun fiber formulations in order to obtain a stable drug release profile. Wu et al. [33] in 2020 investigated how the polymer composition of nanofibers affects the drug release profile. They made two-component electrospun fiber mats through combining PLGA (as the first component) with other polymers with different hydrophilicities (each time one of them used with PLGA as the second component) and Ciprofloxacin (CIP) as the drug. They found that the drug release profile from electrospun fibers contains three stages, each controlled by separate parameters that depend on the polymer composition of the fibers. They determined that fiber swelling, fusion of fibers together and formation of a gel-like structure and polymer degradation are three important parameters affecting the drug release profile from electrospun fiber mats.

Drugs that form stronger interactions with the polymers within the electrospun fiber mats would have a slower release profile. It is difficult to evaluate the variety and intensity of the interactions through laboratory experiments. Thus, all atom MD simulations conducted for the study of electrospun fibers have mostly focused on the evaluation of interactions of loaded drug with polymer matrices [35-37].

Using electrospinning technique, Aytac et al. experimentally encapsulated CIP loaded hydroxypropyl-beta-cyclodextrin (HP β CD) into a gelatin nanofibrous matrix (see **Figure 1**). Then, using MD simulations, they evaluated the interactions of CIP with HP β CD. To obtain the initial conformation for the start of MD simulations, using molecular docking, first they docked CIP into the HP β CD cavity and then, based on the energy of binding, chose the most favorable conformation. In their MD simulations, they observed that Van der Waals interactions are the most significant driving forces in the complexation of CIP with HP β CD. They also observed that Piperazinyl fragment of CIP (the hydrophobic part of CIP), is embedded within the HP β CD cavity [35].

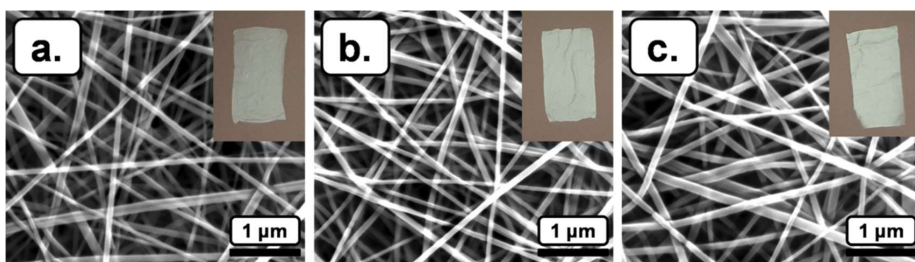


Figure 1. SEM images and photographs (given as insets) of (a) gelatin nanofibers, (b) gelatin-CIP nanofibers, and (c) gelatin-CIP/HPβCD nanofibers. Reprinted from [35] with permission from Elsevier.

Steffens et al. conducted MD simulations on Polyvinyl alcohol (PVA) and Dacarbazine to provide insight over their experimental observations of a burst release of Dacarbazine from PVA fibers within 30 minutes (around 58% in pH 6.8) that is followed by a sustained release for three days. In their MD simulations, they observed that some drug molecules interact with PVA, and some have no interaction with PVA and are only in contact with the solvent. They came to this conclusion that the drug molecules that are only in contact with solvent cause a burst release while those that are complexed with PVA (through different kinds of interactions including hydrogen bonds) will be released more slowly [37].

In study I [38] in this thesis, through combined effort of experiments and MD simulations, we have evaluated how the polymer composition affects drug release from nanofibers.

2.1.1.2. Hydrogels

Hydrogels are polymeric DDSs that swell in water [39] and are made up of highly hydrated (typically 70–99% [39]) polymeric networks (**Figure 2**) formed from natural, synthetic, or semi-synthetic polymers, which are physically or chemically cross-linked [40] (**Figure 3**). Chitosan and hyaluronic acid are examples of natural polymers and PEG and PVA are common synthetic polymers used in hydrogels. Hydrogels can be classified based on cross linking method, physical properties, response to different stimulants, ionic charge, degradability and source of the polymers used in them [41].

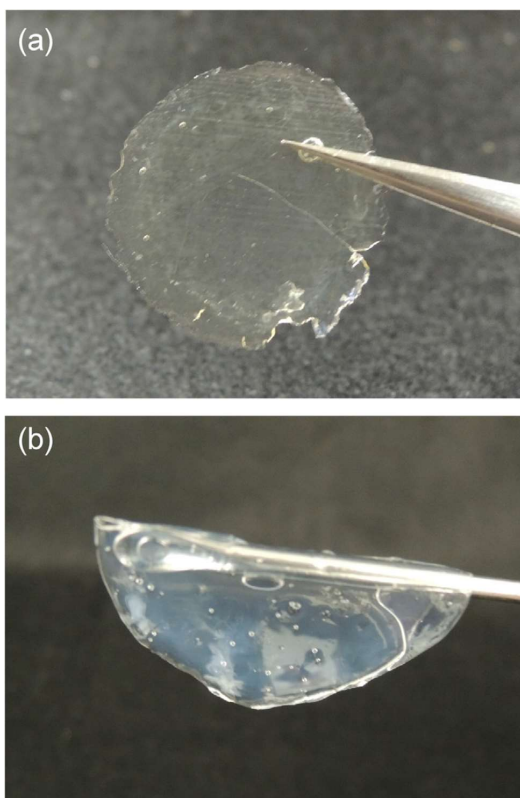


Figure 2. The PEG-grafted chitosan gel sheet: (a) dried gel sheet; (b) hydrated gel sheet. Reprinted from [42] with permission from Elsevier.

Although, due to their high water content, hydrogels are specially suitable for the delivery of hydrophilic drugs [39], various methods could be implemented to load hydrophobic molecules into the hydrogel matrices of which the use of block copolymers with a hydrophobic block such as Poly lactic acid (PLA) or PCL for preparing hydrogels can be named [43]. Hydrogels can be administered through local implantation of the hydrogel inside the body [40]. Therefore, great emphasis has been placed on the development of injectable hydrogels [39]. Injectable hydrogels are of considerable importance as they can minimize the need for surgical implantation, one of the major drawbacks associated with their use as a DDS [44].

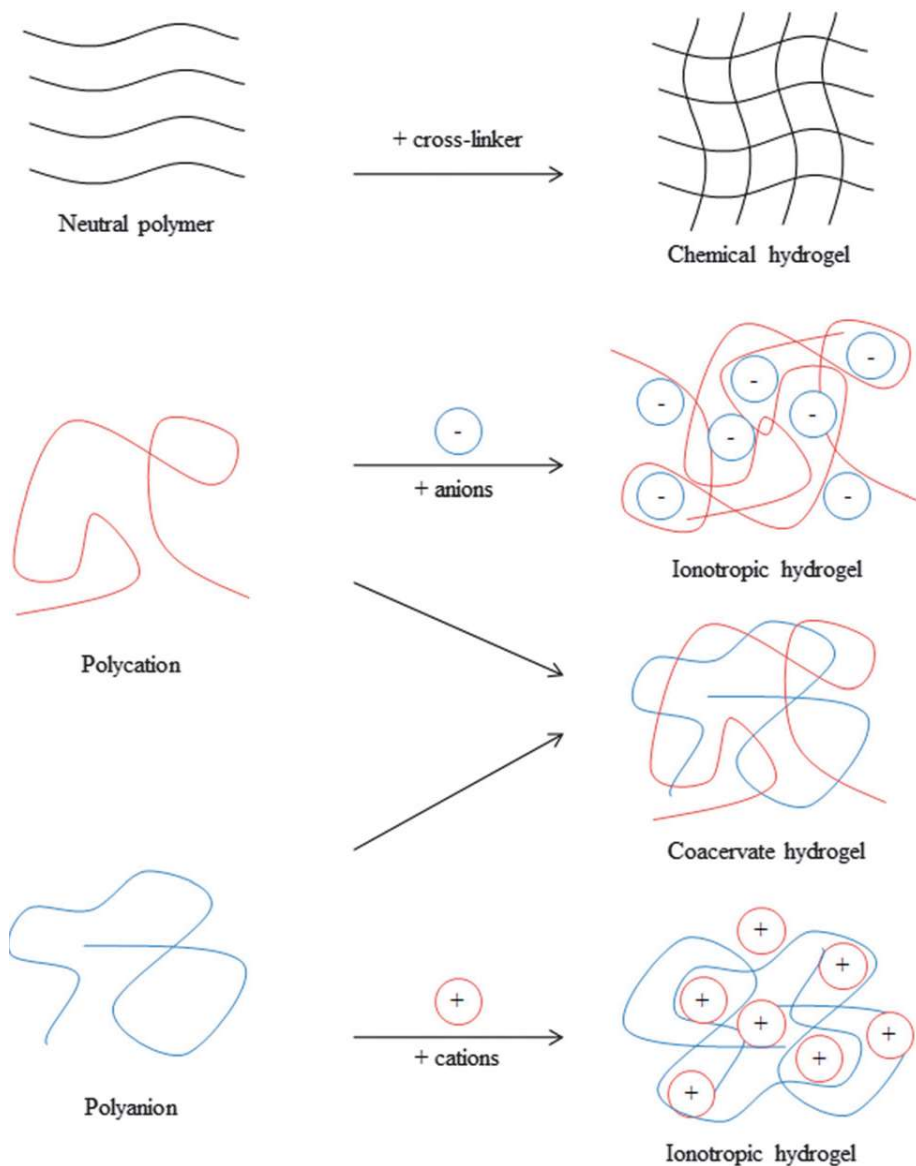


Figure 3. Schematic presentation of different hydrogel-forming mechanisms Reproduced from [45] with permission from the Royal Society of Chemistry.

Hydrogels have been used for drug delivery to lungs, brain, skin, small intestine [44] and also have been widely used for cancer treatment [43, 46]. However, since many of the *in vivo* studies to date examine hydrogels in subcutaneous ectopic tumor models and not in orthotopic tumor models, still

more validation of antitumor results of hydrogel loaded DDSs is necessary [46].

Since the use of MD simulations helps us to gain a deep understanding of the molecular-level structure/property relationships in hydrogels, the use of this tool is crucial to obtain optimized hydrogels [47]. MD simulations have mainly been used for the study of three main characteristics of hydrogels; the behavior of water in hydrogels [48-50], mechanical properties of hydrogels [47, 51] and evaluation of different aspects of the deformation process of hydrogels [52, 53].

The behavior of water in hydrogels is very important as it has a large impact on the properties of hydrogel materials. The behavior of water such as hydrogen bond (H-bond) formation and breaking speed is different in bulk water in comparison to nonbulk environments [54]. Through MD simulations, Sun et al. evaluated the state of water molecules in hydrogel and studied the dynamics of water molecules through calculation of the self-diffusion of water in hydrogels. They determined that water molecules move faster as the hydrogel becomes increasingly swollen [48]. Molecular dynamics simulations confirmed that water content of the hydrogel has a significant effect on the mechanical properties of hydrogels; the hydrogels with a lower water content have enhanced tensile and shear properties [47].

He et al. conducted MD simulations on poly(carboxybetaine methacrylate) (PCBMA) and hydroxylated poly(carboxybetaine methacrylate) (OH-PCBMA) hydrogels to examine how hydroxyl groups -as physical cross-linkers- affect the mechanical properties of the hydrogels. They observed that, due to higher number of inter chain polymeric H-bonds formed within OH-pCBMA hydrogels, the polymer network is enhanced within these hydrogels that results in a higher elastic modulus in OH-PCBMA hydrogels in comparison to PCBMA hydrogels [51].

2.1.2 POLYMERIC NANOPARTICLES

For the intention of systemic administration of polymeric DDSs and especially drug delivery to tumors, polymeric DDSs are formed into nanoparticles. Depending on the method of preparation of polymeric nanoparticles, different kinds of nanoparticles including nanospheres and nanocapsules are produced [55] (**Figure 4**).

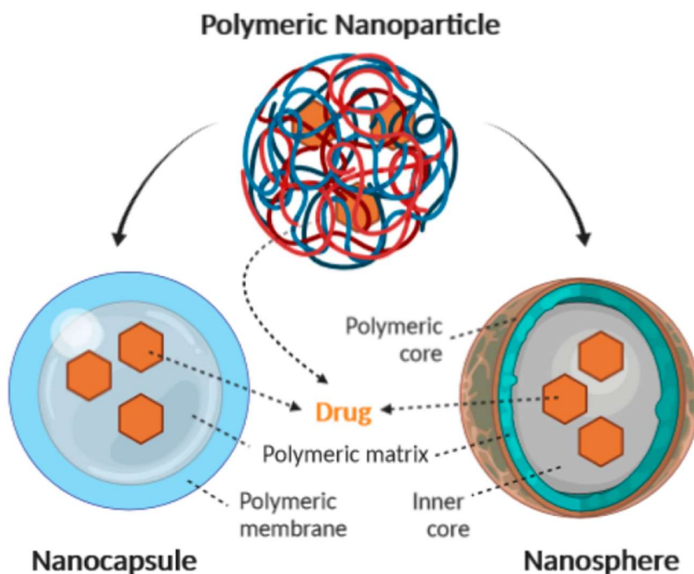


Figure 4. Schematic representation of the structure of nanocapsules and nanospheres (from reference [56]).

Nanospheres are matrix particles that are mostly spherical with a size ranging from tens of nm to a few hundred nm [55] in which the drug is physically and uniformly dispersed [57]. Nanocapsules act like a reservoir (they have a core-shell structure) where the drug is loaded into the core and surrounded by a polymeric shell [55, 57]. PCL, chitosan, PLA and PLGA are examples of polymers used to form nanoparticles [58] (see **Figure 5**).

There are several preparation methods of polymeric DDSs that can be classified into two categories: polymerization of monomers and those taking advantage of preformed polymers [59]. Preformed polymers have been used to a far greater extent, as there are many limitations and problems involved in monomer polymerization that can be avoided using preformed polymers. In

the process of monomer polymerization, surfactants are used to stabilize the resulting particles. Even if a small amount of surfactant is used, surfactant residues remain in the polymer latex that changes the properties of the resulting nanoparticles. The preparation of monodisperse particle size is another challenge in using the monomer polymerization method [60].

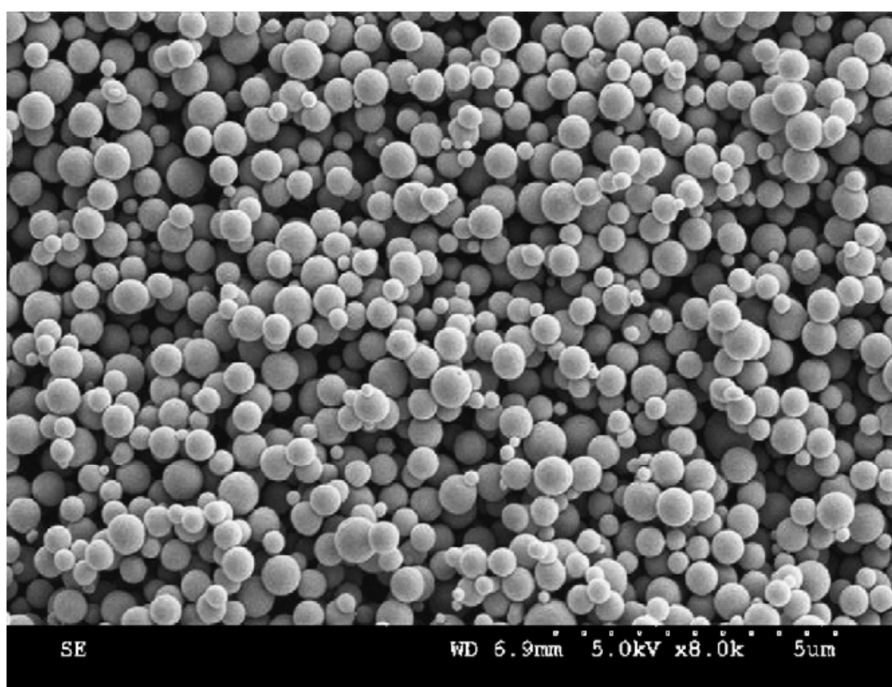


Figure 5. SEM image of PLGA nanoparticles loaded with Ketoprofen. Reprinted from [61] with permission from Elsevier.

The main mechanism used for the formation of polymeric nanoparticles from preformed polymeric chains is self-assembly. Hydrophobically modified water soluble polymers [62-64], amphiphilic block copolymers [65-67] and polyelectrolyte polymers are examples of polymers with self-assembly properties that can spontaneously form polymeric nanoparticles in a suitable solvent [68, 69].

Polymeric nanoparticles can be formed through either one-step or two-step procedures. One-step procedures include nanoprecipitation, dialysis or the

rapid expansion of supercritical fluids. Two-step procedures include emulsification-solvent evaporation and emulsification-solvent diffusion [59].

Size is one of the most important characteristics of polymeric DDSs as it affects several biological phenomena including circulation half-life and passive targeting to tumors through the enhanced permeability and retention (EPR) effect. Since 1986, when the EPR effect was discovered by Maeda and Matsumura [70-74], it has been the guiding principle for cancer nanomedicine development [75]. The EPR phenomenon is based on pathophysiological characteristics of solid tumors such as defective vascular architecture and impaired lymphatic drainage [76]. These features lead to a considerably higher extravasation of nanomedicines in tumor tissues in comparison to normal tissues.

In spite of the fact that there is a considerable literature concerning the use of the EPR effect for the targeting of anti-cancer drugs to tumors, as of yet, a relatively small number of nano DDSs have reached the market. This has caused an intense debate regarding the existence and the extent of the EPR effect [75]. Wilhelm et al. conducted an intensive literature survey of the publications of the last 10 years and observed that, on average, only 0.7% of the dose of the anti-cancer drug administered through nanoparticles were successfully delivered to a solid tumor [77]. From this observation, they concluded that the current underlying principles of nanoparticle targeting that is based on the EPR effect, will not produce the desired clinical outcomes [77].

In response to Wilhelm et al. [77] who conclude that the EPR effect is not an efficient mechanism for targeting solid tumors, Hiroshi Maeda who discovered the EPR effect, wrote an article in 2021 (in the last year of his life) [78] and stated that the EPR effect inefficiency reported in the literature is due to experimental data obtained based on poorly designed nanomedicines. Maeda wrote that most of the examples of failed cases of the nanoparticles using the EPR effect is related to a too short blood circulation time (<3 h) or lack of fulfilling size requirements necessary for the EPR effect that should be larger than 40 KDa to above 250 KDa (>5 nm to 100 nm) to escape renal clearance (>5 nm to 100 nm). He also stated that the type of solid tumor would also affect

the efficiency of the EPR effect as different tumors have different vascular densities and blood flow.

Adequate stability during circulation in the blood (more than 12h), appropriate size, biocompatibility (to escape the immune system), appropriate surface charge and normal blood flow rate are some of the requirements for a nanoparticle to have a significant EPR effect [79]. As discussed, size of the nanoparticles is very important for their application in tumor targeting [80]. In study **IV** [81] in this thesis, we investigated the mechanism through which the temperature at which the nanoparticles are formed affects their size.

MD simulations have been intensively used to study different characteristics of nanoparticulate polymeric DDSs of which the two most studied characteristics are: evaluation of their loading capacity (drug encapsulation) through investigating drug-polymeric carrier interactions [82-87] and evaluation of the mechanisms and driving forces involved in the formation of polymeric nanoparticles [88-90].

Using atomistic MD simulations, Zhang et al. [90] investigated the aggregation behavior of the copolymer poly(oligo(ethylene glycol) methyl ether acrylate)-block-perfluoropolyether (poly(OEGA)*m*-PFPE) based on their fluorine content. They also evaluated the interaction of the polymeric nanoparticles formed from this copolymer with the cell membrane. In this copolymer, PFPE is the hydrophobic segment and OEGA is the hydrophilic component of the copolymer. Molecular dynamics simulations confirmed their previously obtained experimental results that aggregation behavior of this copolymer in solution depends on the fluorine content of the copolymer. They observed that copolymers with lower fluorine content transform into single-chain folded nanoparticles while copolymers with higher amounts of fluorine content, would make multiple-chain nanoaggregates. To evaluate the interaction of nanoparticles with the cell membrane, they placed nanoparticles at a 5Å distance from the surface of 1-palmitoyl-2-oleoyl-sn-glycero-3-phosphocholine (POPC) membrane containing stochastic protrusion of the tail of one of the POPC molecules (oriented toward the solution). The reason they used a membrane with protrusion for their simulations was that already Van Lehn et al [91, 92] observed using MD simulations that following contact

between protruding solvent-exposed lipid tails and amphiphilic nanoparticles, fusion between them occurs. Zhang et al. observed that while multi chain aggregates only remained on the surface of the membrane, single chain aggregates insert and fuse within the lipid membrane. They concluded that although single chain aggregates contain fewer hydrophobic PFPE segments in comparison to multi chain aggregates, their hydrophobic segment makes stronger hydrophobic interactions with the membrane exposed lipid tail as the hydrophobic PFPE segment in single chain aggregates is more exposed to the solution and consequently to the membrane surface.

2.2 LIPIDIC DRUG DELIVERY SYSTEMS

So far the most successful lipid drug delivery system in pharmaceutical sciences are liposomes. The first liposomal formulation approved by the FDA was Doxil®. It is a PEGylated liposomal formulation encapsulating Doxorubicin that is used for cancer treatment. In 2017 FDA approved Vyxeos® for cancer treatment as the first liposomal product encapsulating two anti-cancer drugs (Cytarabine and Daunorubicin) [93].

The main building block of liposomes is phospholipids. Phospholipids are amphiphilic molecules that have a hydrophilic head and two hydrophobic chains. The head groups of phospholipid molecules may be neutral, positive, or negatively charged. The head groups with positive charge have been used to a greater extent in preparation of liposomes in comparison to neutral and negatively charged head groups as they demonstrate more cellular uptake and can be used for delivery of biological macromolecules with negative charge like DNA [17]. Different derivatives of Phosphatidylcholine (lecithin) and phosphatidylethanolamine (cephalin) are among the most used phospholipids for the preparation of liposomes [94]. For example, 1,2-Distearoyl-sn-glycero-3-phosphocholine (DSPC) and 1,2-Dioleoyl-sn-glycero-3-phosphoethanolamine (DOPE), are two synthetic derivatives of phospholipids that frequently used in combination with other lipids for the preparation of liposomes [95]. Depending on different parameters including the temperature (liposomes are only obtained at temperatures above the gel to liquid crystalline

transition temperature of phospholipids [96]) and the molecular shape, upon contact with water, phospholipids spontaneously self-assemble into different colloidal particles (**Figure 6**) [97]. This rearrangement of phospholipids is entropically favored, as it reduces non-favored interactions in water [96]. These self-assembled structures remain stable through both Van der Waals forces that keep the long hydrocarbon tails together and hydrogen bonds and polar interactions between the water molecules of the aqueous environment and the polar head groups of lipids [98].

Depending on the method that is used for the preparation of liposomes (that mainly are classified as solvent free methods and solvent displacement methods), liposomes with different diameters and lamellar properties are obtained with small unilamellar vesicles in the size range of 20–100 nm [96] as the most important [94] regarding drug delivery applications. Depending on the phospholipids that are used, the bilayer thickness of liposomes is 3–5 nm [96].

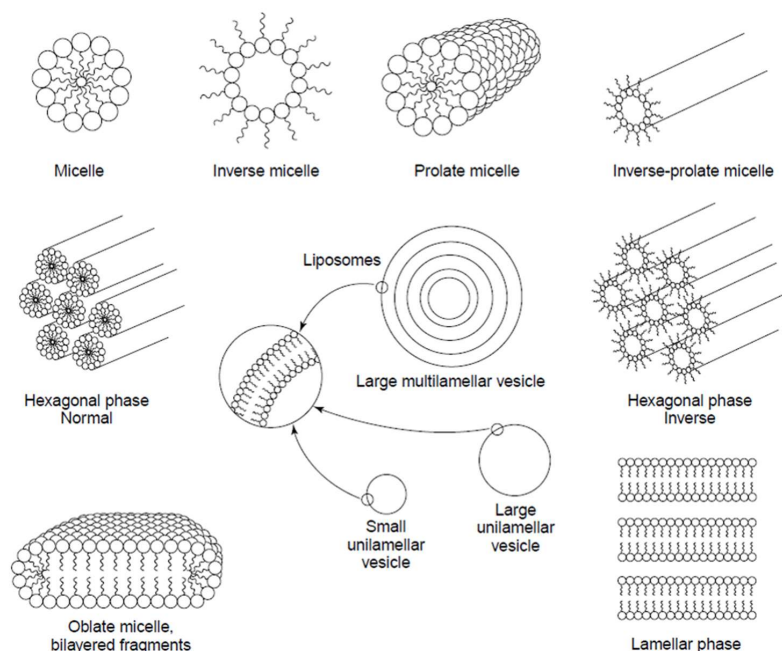


Figure 6. Different structures may be formed due to Self-aggregation of phospholipids. Reprinted from [97] with permission from Elsevier.

The most important concern regarding the preparation of liposomes is their stability [95]. Liposomes may encounter both chemical and physical instability. Oxidation of fatty acid chains and hydrolysis of ester moieties are two examples of chemical instability of liposomes. Therefore, it is recommended that liposomes are stored under an inert gas at low temperature [96]. When physical instability of the liposomes is discussed, it is meant that their number, size and structure change in the course of time [96] for example liposomal aggregation and fusion occur [95]. Physical stability of liposomes is mainly controlled by their phase behavior. The phase behavior of liposomes is very important regarding drug delivery applications as it affects the drug release profile. Depending on the lipids that are used in the composition of liposomes, when the temperature goes below the transition temperature of the lipids, two scenarios are possible: 1- the liposomes may change into other colloidal structures (this will be discussed in detail in section 2.2.2) 2- the overall structure of liposomes is preserved and just a liquid crystalline to gel phase transition occurs. To make liposomes physically more stable, some other compounds such as Cholesterol [95, 98] and PEG [95] is added to the composition of liposomes. In study II [99] in this thesis, we have evaluated how attachment of PEG affects the stability of liposomes.

2.2.1 PEGYLATED LIPOSOMES

Although DDSs have demonstrated promising results, there is still a long way ahead to show their best performance [100]. As it was discussed in section 2.1.2, one of the challenging issues hampering the efficiency of nanoparticles is their rapid clearance from the blood stream. Upon systemic administration, 99% of the administered nanoparticles are removed from blood circulation. This is mainly performed by the mononuclear phagocytic system (MPS) (also known as the reticuloendothelial system). Different organs are involved in MPS with the liver and spleen as the most important. There are macrophages and phagocytic cells in these organs that detect foreign materials and then take them up [77]. This is one of the reasons many liposomes have shown good results *in vitro*, but they fail to be successful *in vivo* [17].

It is almost thirty years since the time it was determined that the process of phagocytosis of particles by macrophages is triggered by opsonization where particles are coated with different proteins (see **Figure 7**) from the complement system that are recognized by receptors on the surfaces of macrophages [101].

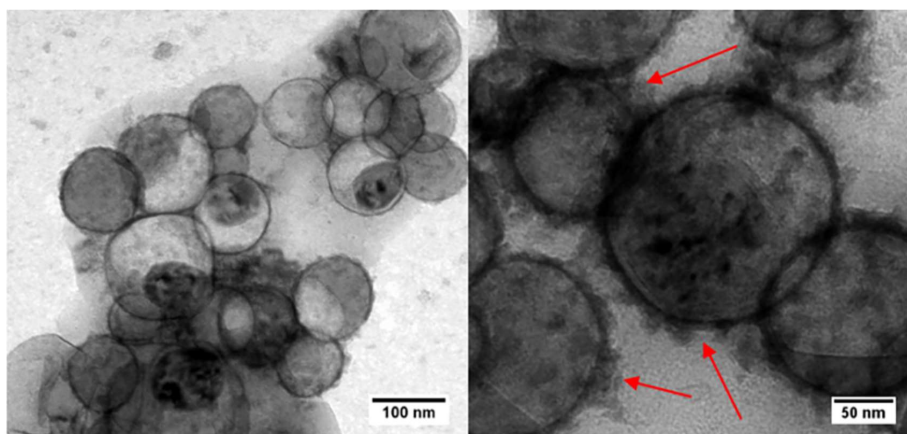


Figure 7. TEM images of liposomes incubated with plasma. The arrows indicate protein corona formation (from reference [102]).

Since most of the liposomal products (84%) that are currently under clinical trials are administered via the intravenous route [103] they should be properly optimized for encountering the MPS. First-generation liposomes (classical or conventional liposomes) that are without any surface modifications [104], are rapidly removed from the blood stream and accumulate in the liver and spleen [103]. This shortcoming of conventional liposomes hindered their preclinical and clinical applications [104]. As a solution, a new generation of liposomes with the name of “stealth liposomes” was developed.

Stealth liposomes are liposomes with hydrophilic polymer chains (most commonly PEG) functionalized to the headgroups of the lipids from which they are composed. Although it is widely accepted that surface modifications of liposomes with PEG significantly increase the blood circulation time of liposomes [105], the mechanism through which PEG helps nanoparticles to escape from the MPS is still not fully understood. While some believe PEG hinders protein interaction with the liposome surface [105-107], Weber et al.

found that PEGylation does not significantly alter the protein corona [102]. On the other hand, Moghimi et al. believe that PEG has no role in helping nanoparticles to escape from the MPS and prolongation of the circulation time of PEGylated nanoparticles is due to saturation of opsonization system [108]. However, the theory of Moghimi et al. is challenged as particles decorated with other hydrophilic polymers are not as effective as PEG in helping nanoparticles to escape the MPS.

It seems that the conflicting results regarding the mechanism that PEGylated nanoparticles use to stay longer in blood circulation is due to the fact that different experimental methods, animal models and variables have been used in the analysis by different groups [109]. For example, Palchetti et al. [110] found that in comparison to PEGylated liposomes that are statically incubated in a protein solution in vitro (as the method many groups have used so far to study protein interactions with PEGylated liposomes), when PEGylated liposomes are circulated in the same solution under a dynamic flow, a wider variety of protein species would be detected in the protein corona on the surface of particles and also the particles are more negatively charged.

During the last ten years, our group (pharmaceutical biophysics) in the faculty of pharmacy of the University of Helsinki has contributed to conducting experimental studies [111] and all-atom MD simulations [112-116] on PEGylated membranes to evaluate the effect of PEG on characteristics of liposomes. Since it is experimentally proved that the surface charge of nanoparticles affects their interaction with the complement system, evaluation of the effect of PEGylation on the surface charge of liposomes is very important as it may shed light on the mechanism through which PEGylated liposomes can evade uptake by the MPS. Through conducting MD simulations on PEGylated phospholipid membranes Magarkar et al. determined that among three physiologically relevant cations that were considered in the simulations (Na^+ , K^+ and Ca^{2+}) PEG makes the strongest interaction with Na^+ and then K^+ and it make no interaction with Ca^{2+} [113]. Stepniewski et al. observed that interactions of Na^+ with PEG is so strong that each Na^+ binds to about five oxygen atoms of PEG forcing the PEG chain to loop around it [112]. Magarkar et al. also observed that Cl^- ion penetration extent in the PEG layer decreased

as the ratio of PEGylated lipids in the membrane increased which consequently lead to a positively charged PEG layer [113].

In addition to the effect of PEG on the circulation time of liposomes, it also affects the structural stability of liposomes. In a study conducted by Dutta et al. [117] in 2021, for the first time all-atom MD simulations was used for finding a rational approach for the design of thermo-sensitive PEGylated liposomal formulations. To obtain their aim, they compared phase behavior of pure 1-palmitoyl-2-stearoyl-sn-glycero-3-phosphocholine (PSPC) membranes with membranes containing PSPC and DSPE-PEG2000 at seven different temperatures (280, 300,310,320, 330, 340 and 360 K). They compared bilayers regarding four structural aspects: area per lipid, bilayer thickness, deuterium order parameter of PSPC acyl chains and torsional distribution of the lipid tails. They observed that the presence of PEG in the structure of PSPC bilayers, reduces the gel to the liquid crystalline phase transition temperature as much as around ten degrees. They also observed that the PEG penetrates into the lipid bilayer even when the bilayer is in the gel phase causing distortion in the typical gel phase structure. However, it is necessary to point out that the lack of using cholesterol in the bilayers they studied, might have affected both the phase behavior and structural properties they reported.

Although PEG remains as the gold standard for the protective polymer stealth sheath of liposomes [18], there are three challenges in using it. It is reported that PEG prevents the liposomes from being captured by the target cells [18], PEG induces a significant immune response known as the accelerated blood clearance (ABC) phenomenon, when repeatedly injected [118-120] and it reduces the pH-sensitivity of pH-sensitive liposomes [121, 122]. Therefore, the new research on PEGylated liposomes focuses on attaching PEG to liposomes in a removable manner for example attaching PEG to liposome lipids through cleavable bonds like pH-sensitive hydrazine and ester linkages [123].

2.2.2 PH-SENSITIVE LIPOSOMES

The drug delivery mission of liposomes ends when the drug is successfully released from them into the cytoplasm of the target cells. One of the most successful strategies taken in this regard has been the use of pH-sensitive liposomes where the liposomes are stable at physiological pH (pH 7.4) but undergo lamellar to inverted hexagonal (HII) phase transition thus destabilized under acidic conditions inside lysosomes leading to the successful release of their payload into the cytoplasm [124]. In the HII phase, lipids are arranged in a hexagonal geometry and form lipid tubules. Head groups of lipids are oriented toward the interior of the tubules where it is filled with water and ions (see **Figure 8**).

Among all classes of pH-sensitive liposomes that have been proposed so far, the most mature technology is preparation of these liposomes through the blending of phosphatidylethanolamine (PE) derivatives with a stabilizer [18]. Stabilizers are amphiphilic molecules containing an acidic group (for example, carboxylic group); its protonation in acidic pH triggers the destabilization of liposomes. Cholesteryl hemisuccinate (CHMS) is the most popular amphiphilic stabilizer used extensively in the preparation of pH-sensitive liposomes in combination with PE lipids [125, 126].

Among different PE lipid derivatives, DOPE is the main phospholipid used in building pH-sensitive liposomes [124, 127]. The small size of the DOPE head group and formation of intermolecular H-bonds between amine and phosphoryl groups of adjacent DOPE molecules increases the tendency for DOPE bilayers to undergo a lamellar-to- HII phase transition [128].

DOPE lipids can form into stable liposomes only when the pH is above 9.0 where PE is negatively charged [129] however, in neutral pH, they do not form into stable bilayers. At physiological pH, CHMS is deprotonated and is negatively charged [130] and its presence with DOPE lipids stabilizes them into the lamellar phase [131]. When liposomes enter the lysosomes inside the cytoplasm of the cells where pH is dramatically reduced, CHMS again is protonated. This will lead to the destabilization of liposomes and consequently drug release from them. In study **III** [132] in this thesis, we have evaluated the

mechanism of action of CHMS in stabilizing and de stabilizing pH-sensitive liposomes.

Since the structural properties of lipids in the HII phase affects the release of their payload [133], these properties have already been studied experimentally [134-138]. However, experimental evaluation of these properties encounters many challenges, for example low resolution and difficulty of study of HII phase structural properties while considering multiple parameters such as temperature and hydration at the same time. This is the reason that in 2020, Ramezanzpour et al. [139] published an interesting article where using MD simulations, they evaluated how the change in the hydration level and temperature would affect the structural properties of DOPE lipids in the HII phase. They managed to successfully calculate different structural properties of DOPE lipids in the HII phase including radius of the water core (R_w) and the lattice plane distance (d_{hex}) (see **Figure 8**), with a great agreement with the available experimental data.

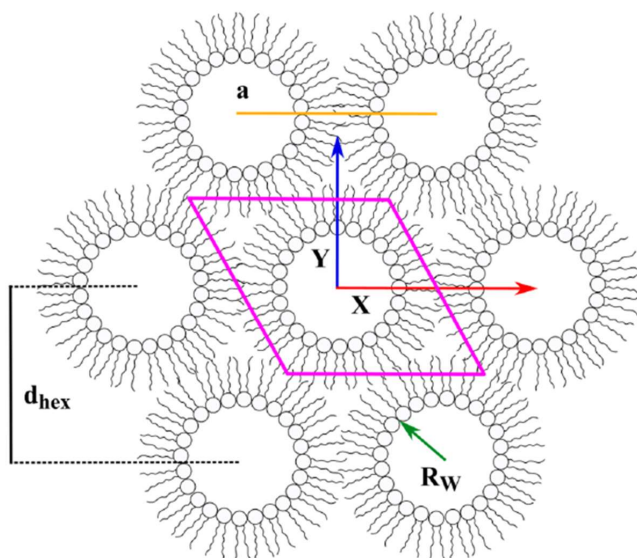


Figure 8. DOPE lipids in the HII phase. Lipid tubules are perpendicular to the XY plane. The radius of the water core (R_w), lattice plane distance (d_{hex}), and lattice spacing (a) have been shown in the figure (from reference [139]). Reprinted with permission from *Langmuir* 2020, 36, 24, 6668–6680. Copyright 2020 American Chemical Society.

For example, they calculated a value of 20.01 Å for R_w of DOPE in 303K (while considering 16 water molecules inside the lipid tubule) which was in agreement with the obtained experimental R_w value (~ 20 Å). To calculate the value of R_w , Ramezanzpour et al. used the probability distribution of P atoms of DOPE lipids with respect to the lipid cylinder axis.

3 AIM OF THE THESIS

The general objective of this PhD thesis was the use of all atom MD simulations for the study of DDSs. Two polymeric and two lipidic DDSs were studied using all atom MD simulations. In each of these studies, a specific property of DDSs was evaluated in detail including drug release profile (study **I**), stability (study **II**), pH-sensitivity (study **III**) and size (study **IV**). In studies **I, II and IV**, the all-atom MD simulations were performed alongside complementary experiments our experimental colleagues performed and in study **III**, the MD simulations were compared with previously available experimental results.

The specific aims of each study are as follows:

1. Investigating the interactions of chloramphenicol with PCL and PEG In order to obtain further insight into the factors affecting the release of the drug from electrospun polymer matrices (study **I**)
2. Evaluation of the effect of different PEG polymers on the stability of liposomes. PEG differences were related to the anchoring moiety (DSPE, Cholesterol, and Cholane), PEG molecular weight (2 kDa and 5 kDa) and PEG shape (linear and branched PEG) (study **II**).
3. Providing insight into three questions regarding pH-sensitive liposomes (a) why incorporation of PEG into DOPE-CHMS liposomes reduces their pH-sensitivity; (b) How CHMS in its anionic form stabilizes DOPE bilayers into a lamellar conformation at a physiological pH of 7.4 and (c) how the change from CHSa (Deprotonated (anionic) form of Cholesteryl hemisuccinate) to CHS (Protonated (neutral) form of Cholesteryl hemisuccinate) at acidic pH triggers the destabilization of DOPE bilayers (study **III**)
4. Evaluation of the mechanisms that lead to the formation of chitosan-phosphorylated Glucan particles with a smaller size as temperature increases (study **IV**).

4 OVERVIEW OF THE METHODS

4.1 COMPUTATIONAL MODELLING OF DRUG DELIVERY SYSTEMS

The limitations to the extent to which mechanistic insight can be gained from experiments has resulted in the process through which novel DDSs are developed to be mostly based on a process of trial and error. This can be compensated by computational modelling techniques that provide detailed information regarding molecular interactions of drugs and carriers [140]. Computational modelling can be conducted at different levels of detail. In the most detailed computational modelling, the system is described by Quantum Mechanical calculations. This method has been for example used for the study of DDSs made up of carbon nanotubes, however, in practice this method is not applicable to large DDSs with a high number of degrees of freedom and solvated systems [140].

The next level of detail is obtained using molecular mechanics methods also known as force field methods [141]. The molecular mechanics concept is based on a combination of empirical physical chemistry based rules with the insight from the quantum mechanical interactions of atoms [142]. In molecular mechanics several assumptions are considered, for example the Born-Oppenheimer approximation where the electronic motions are ignored and the energy of a system is only calculated as a function of nuclear positions [141]. Molecular dynamics simulation alone or in some cases hybridized with Monte Carlo (MC), use the molecular mechanics paradigm for the study of biological systems. Through these methods, atomistic simulations can be used as a model to study the actual systems [143].

Both the MD and MC methods would calculate most of the thermodynamic properties of the system such as pressure and internal energy however, the accurate determination of some other thermodynamic properties such as entropy and free energy by MD and MC are difficult [141] and additional techniques such as MM/PBSA (molecular mechanics with Poisson-Boltzmann

and surface area solvation) [144], thermodynamic integration or use of methods with a force bias including umbrella sampling [145] are necessary.

4.2 MOLECULAR DYNAMICS SIMULATIONS

In MD simulations, the real dynamics of the system is evaluated where the time average of the properties of the system are calculated in a way that each new system configuration depends upon previously visited configurations [141]. Atomistic MD simulation facilitates the interpretation of experimental data at the atomic level [146] and can, alongside experimental analysis, assist the rational design of new formulations of DDSs with improved efficacies [140]. Molecular dynamics simulations can be seen symbolically, as a computational microscope where biomolecular mechanisms that are difficult to be observed by present experimental techniques can be elucidated [147]. During the last forty years, MD simulation has advanced from simulating several hundreds of atoms to entire proteins in solution and large polymeric complexes. The use of high performance computing (HPC), and the simplicity of the basic MD algorithm are two reasons for this remarkable improvement. The algorithms are used to generate enough simulation data to draw statistically valid conclusions about the behavior of the system of interest. This data is also used to calculate thermodynamic properties of the system through statistical mechanics [140].

To conduct MD simulations, researchers may use any of the following software packages, including GROMACS [148], NAMD [149], CHARMM [150] and AMBER [151], all of which are compatible with the messaging passing interface (MPI) and the use of graphical processing units (GPUs) both speeding up the process of MD simulations. In this thesis, all atom MD simulations and evaluation of atomistic interactions were conducted using the Gromacs package. Nowadays, simulation on GPUs alone or combined with MPI, is the default strategy to improve the performance of atomistic MD simulations [143].

4.2.1 PERIODIC BOUNDARY CONDITIONS

An important issue that should be considered while conducting MD simulations is that the boundaries of the simulation box are correctly treated. The classical way to minimize edge effects in a finite system is the use of periodic boundary conditions [152] where particles experience forces as if they are in bulk fluid enabling us to use a relatively small number of particles for the calculation of macroscopic properties of the system. When periodic boundary conditions are implemented, the simulation box (unit cell) is surrounded by an infinite number of similar image boxes in space. This makes it possible that if a particle leaves the simulation box during MD simulation, then, its image enters to the box from the opposite side [141]. In Gromacs, while using periodic boundary conditions, minimum image convention is implemented meaning that for the short range non-bonded interaction terms, only the nearest image of the other particles are taken into consideration. However, to calculate non-bonded interactions as accurately as possible, the PME method is implemented by Gromacs for the calculation of long-range electrostatic and Van der Waals interactions (only the attractive term of the LJ potential) [152]. When using periodic boundary conditions, the cutoff should not be more than half the length of the simulation box so that a particle does not see its own image [141].

4.2.2 DIFFERENT STAGES OF MD SIMULATIONS

The MD simulation is conducted in four stages. It starts with building an initial configuration of the system that is obtained from experimental structures or comparative modelling data. Then, following energy minimization, an equilibration phase is conducted during which the system evolves from the initial conformation. During this stage, thermodynamic and structural properties of the system are monitored to assure the system achieves stability. Next, the production phase starts where the data for later analysis of MD simulations is collected. Last and in fact the fourth stage is analysis of data obtained in the production phase [141].

During the equilibration and production phase, to calculate the forces, first potential energy U is calculated using the parameters set in the force field. Then, forces acting on a certain atom i is derived from the negative gradient of the potential energy.

$$\vec{f}_i = -\nabla U_i(\vec{r}) \quad (3.1)$$

Then, by solving the differential equations embodied in Newton's second law ($F = ma$), accelerations of the particles can be obtained.

$$\vec{a} = \frac{d^2\vec{r}_i}{dt^2} = \frac{\vec{f}_i}{m_i} \quad (3.2)$$

With knowledge of the accelerations of the atoms, using positions and velocities at a time t the positions and velocities at a time $t + \Delta t$ is calculated [141]. Every time the positions and velocities of the atoms in the system are renewed, they can be saved in a trajectory file enabling the user to generate a data file of configurations in time with every degree or nearly every degree of freedom of atoms considered that can be used for analysis [140].

Equations of motion are integrated using integrating algorithms upon this assumption that the positions, velocities, and accelerations can be approximated as Taylor series expansions. The most important features of an ideal integrating algorithm is to conserve energy and momentum and to work properly with a long time step (Δt). The verlet algorithm and its variations are the most widely used integrators of equations of motion in MD simulation. The Verlet algorithm has some disadvantages one of them is the lack of an explicit velocity term that makes calculation of velocities difficult. Therefore, several variations of the Verlet algorithm such as velocity Verlet algorithm and leap-frog algorithm have been developed [141]. The leap-frog algorithm that is shown in the equations 3.3 and 3.4 is named as such since the velocity of each particle is calculated at half time steps whereas the position is computed at full steps.

$$\vec{r}_i(t + \Delta t) = \vec{r}(t) + \Delta t \vec{v}_i \left(t + \frac{1}{2} \Delta t \right) \quad (3.3)$$

$$\vec{v}_i \left(t + \frac{1}{2} \Delta t \right) = \vec{v}_i \left(t - \frac{1}{2} \Delta t \right) + \Delta t \vec{a}(t) \quad (3.4)$$

The time step significantly affects the rate of MD simulation. The use of constraining algorithms such as SHAKE [153] and LINCS [154] allows us to use longer time steps as these algorithms freeze out the vibrations of bond stretches of hydrogen atoms by constraining these bonds to their equilibrium value.

In MD simulations, the energy of the system is demonstrated by the Hamiltonian as a sum of kinetic and potential energy.

$$H = k + U(\vec{r}) \quad (3.5)$$

k is the kinetic energy of the system and $U(\vec{r})$ is the potential energy as a function of atomic positions. The potential energy is the sum of bonded and non-bonded energy terms that is calculated using the potential energy function that will be discussed in detail in the next section. The total kinetic energy is calculated as the sum of velocity and mass of each atom and as it will be discussed in detail in the next section, will be used for calculation of the temperature of the system:

$$k = \frac{1}{2} \sum_{i=1}^N m_i \vec{v}_i^2 \quad (3.6)$$

4.2.3 ENSEMBLES, THERMOSTATS AND BAROSTATES IN MD SIMULATION

By default, MD simulations are based on integrating the classical (Newtonian) equations of motion for a molecular system in a microcanonical or NVE ensemble (as it is defined in statistical mechanics) [155] where E: the total

energy, V : the volume, and N : the number of the particles will remain constant during simulation. The results obtained from simulations in NVE conditions are not comparable with the experimental results as laboratory experiments are usually carried out at constant temperature and pressure [156]. For the comparison with the experimental results, canonical (NVT) and isothermal-isobaric (NPT) ensembles are more appropriate.

In an NVT ensemble, instead of total energy being constant, temperature is instead conserved (as will be described below) and the total energy of the system fluctuates. To control the temperature in the canonical ensemble MD simulations, the physical system is in contact with a large external system that is named heat bath [156]. The absolute temperature T is obtained from the total kinetic energy through equation 3.7 [152] where k_B is the Boltzmann's constant and N_{df} is the number of internal degrees of freedom of the system.

$$k = \frac{1}{2} N_{df} k_B T \quad (3.7)$$

To control the temperature in NVT ensemble MD simulations, thermostats are used. The thermostat couples a fictitious heat bath to the system [157] with the purpose of maintaining the average temperature constant and generating a thermodynamical ensemble at constant temperature [155]. This coupling is commonly achieved by altering Newton's equations of motion or the particle velocities themselves during the simulation (and therefore can have unintended effects on the system's dynamics and thermodynamics). A thermostat should, ideally a) maintain the correct kinetic energy distribution b) operate in a way that minimally disturbs the Newtonian dynamics c) provides an ergodic dynamics (provides the condition that all states with the same energy are visited with equal probability in the long time limit) [157].

Different methods have been developed to run isothermal MD simulations; the difference between them is related to the method they use to connect the physical system to the heat bath [156]. Three important methods are stochastic-coupling method, Velocity scaling method and extended-system method. The Andersen thermostat uses the stochastic-coupling method where at each time step in the simulation a subset of atoms are randomly selected

and their velocities are stochastically reassigned with a stochastic noise term [157]. Since the Andersen thermostat randomizes velocities, when strongly coupled, it significantly disturbs the velocity time correlations leading to dampening dynamics of the system in comparison to results obtained from MD simulations under NVE conditions (which provide a measure of the true dynamics obtained with the unaltered equations of motion) [157]. The Andersen algorithm is non-smooth meaning that the randomly occurring collisions may interfere with the natural dynamics of the system through generating a discontinuous velocity trajectory [155].

The Berendsen thermostat uses the velocity scaling method to control the temperature [157]. This thermostat, in certain time steps of the simulation (depending on the coupling time constant), multiplies the velocities of all the particles in a system by the scaling factor demonstrated in equation 3.8 where T_o is the temperature of the thermal bath, Δt is the time step, τ is the coupling time constant and T is the instantaneous temperature [158].

$$\lambda = \left[1 + \frac{\Delta t}{\tau} \left(\frac{T_o}{T} - 1 \right) \right]^{\frac{1}{2}} \quad (3.8)$$

The Berendsen thermostat performs the temperature relaxation through the weak coupling method and is considered smooth and deterministic, but it does not reproduce canonical ensemble well [155] since the resulting particle velocities do not have the correct fluctuations i.e. the Maxwell-Boltzmann distribution. Therefore, it is preferable to use it only during the equilibration phase as it moves through conformation space quickly and the coupling parameter can be tuned and changed at different times of equilibration. In the production phase, it is preferred to use other thermostats such as the Nosé-Hoover and V-rescale thermostats. The Nosé-Hoover thermostat performs temperature relaxation by the extended-system method [155] which adjusts velocities by coupling the equations of motion to extended dynamical variables [157]. However, this thermostat can demonstrate non ergodic behavior [159]. The V-rescale thermostat is an extension of the Berendsen thermostat to which a properly constructed random force is added. This thermostat samples the

canonical ensemble considering the assumption of ergodicity and can be used to sample the NPT ensemble when combined properly with a barostat [159].

A barostat is needed in addition to a thermostat for simulating the NPT ensemble. Keeping the average value of the pressure of the system constant is not an easy task as there are more fluctuations in pressure in comparison to other quantities of the system such as the total energy [141]. Barostats try to keep the pressure value constant through implementing different methods such as scaling the volume of the simulation cell or coupling the system to a pressure bath analogous to temperature bath [141].

There are different barostats used in MD simulations to control the pressure of the system two common ones are Brendsen [160] and Parrinello-Rahman [161]. Berendsen barostat tries to keep the average pressure constant through scaling coordinates and box vectors in every step of the MD simulation [152]. Although it is stated that Brendsen barostat does not produce a thermodynamically true NPT ensemble [152] however, it acts very well in scaling a box at the beginning of the MD simulation [152]. In the equilibration phase, it is preferred that Parrinello-Rahman barostat is used as it produces the true NPT ensemble [152]. Parrinello-Rahman barostat uses Extended-ensemble pressure coupling approach where the equations of motion are involved in the mechanism of pressure control [152]. Therefore, the choice of integrating algorithm would affect the quality of the pressure control by the Parrinello-Rahman barostat. Parrinello-Rahman barostat is not a suitable barostat to be used in the beginning of the MD simulation when the pressure is very far from equilibrium as it may result in very large box oscillations and even crash of the simulation [152].

4.2.4 FORCE FIELDS

In the force fields, potential energy is expressed as an empirically parametrized analytical function of the atomic cartesian coordinates [162]. The potential energy U of the system is calculated as the sum of a set of

equations that correspond to bonded and non-bonded interactions (see **Figure 9**). Each force field uses its own parameter values for the calculation of bonded and non-bonded energy to describe the molecular mechanics of molecules [163] in a way that reproduces the closest results to experimental properties of molecules including heats of formation and vibrational frequencies [164]. The choice of the force field has a critical effect on results obtained from an MD simulation as it contains potential energy functions and parameters used for calculating them.

$$U_{total} = \underbrace{U_{bond} + U_{angle} + U_{Pdihedral} + U_{Idihedral}}_{\text{Bonded interactions}} + \underbrace{U_{LJ} + U_{PC}}_{\text{Non-Bonded interactions}}$$

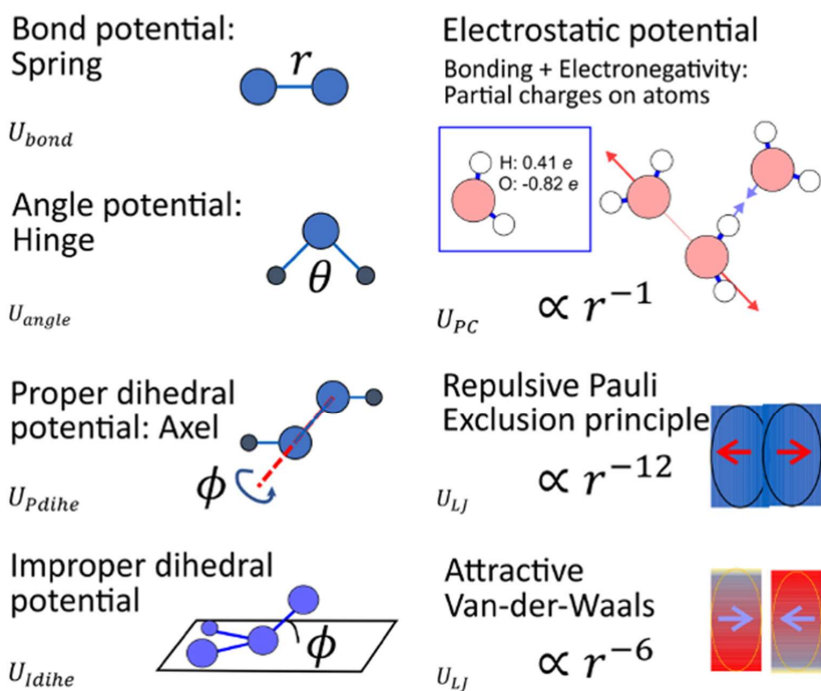


Figure 9. The set of intra and inter molecular interactions used for the calculation of potential energy in molecular mechanics (from reference [142]).

Although equations used in force fields look complicated, they are computationally straightforward to be calculated assuring that energy and force calculations are extremely fast even for large systems [143]. There are different force fields available that can be used with MD engines for example OPLS-AA [165], GAFF [166] and CHARMM [167]. However, while parametrizing molecules that are going to be simulated, one should be careful that force fields should not be mixed as different force fields have been parametrized in different ways. Therefore, parameters of different force fields are not necessarily interchangeable. The choice of a suitable force field for simulation of a particular molecule depends on many factors including the availability of the atom types related to the chemical structure of the molecule in that force field.

4.2.4.1 Bonded interactions

Bonded interactions define molecule structure and are those between covalently bound atoms. Therefore, they are computed based on a fixed list of atoms. Bonded interactions include bond-stretching, angle-bending and dihedrals.

Bond-stretching

The bond stretching between two covalently bonded atoms i and j is represented by a harmonic potential where k^b is the force constant and b^0 is the equilibrium bond length between atoms i and j [152].

$$V_b(r_{ij}) = \frac{1}{2} k_{ij}^b (r_{ij} - b_{ij}^0)^2 \quad (3.9)$$

Bending potential

The angle among three atoms i, j and k can be demonstrated by a harmonic potential on the angle θ_{ijk} where k^θ is the angle force constant and θ_0 is the equilibrium angle [152].

$$V_a(\theta_{ijk}) = \frac{1}{2} k_{ijk}^\theta (\theta_{ijk} - \theta_{0\,ijk})^2 \quad (3.10)$$

Proper dihedrals

The proper dihedral (ϕ) between four atoms i, j, k and l is defined as the angle between the ijk and the jkl planes and is calculated using the equation (3.11) where k_ϕ is the dihedral angle force constant and ϕ_0 is the equilibrium dihedral angle.

$$V_d(\phi_{ijkl}) = k_\phi(1 + \cos(n\phi - \phi_0)) \quad (3.11)$$

Improper dihedrals

Improper dihedrals have different usages one of them is to keep planar groups like aromatic rings planar. As it is shown in equation 3.12, the simplest improper dihedral potential can be demonstrated as a harmonic potential where the improper dihedral angle (ξ) is defined as the angle between the ijk and the jkl planes .

$$V_{id}(\xi_{ijkl}) = \frac{1}{2}k_\xi (\xi_{ijkl} - \xi_0)^2 \quad (3.12)$$

4.2.4.2 non-bonded interactions

Non-bonded interactions of the system include Van der Waals and electrostatic interactions. Energy of the Van der Waals interactions is calculated using the Lennard-Jones potential (U_{LJ}) function and energy of short-range electrostatic interactions (U_C) is calculated using Coulomb's law. The non-bonded interactions are calculated within a certain radius on the basis of a neighbor list.

Lennard-Jones potential

This potential describes the Van der Waals energies where the tendency of atoms to repel and attract one another regarding the inter nuclear distance is calculated [164]. Several potential functions like Buckingham potential or Hill potential have also been proposed for the description of Van der Waals energies however, the U_{LJ} 12-6 function still is the best known [141] :

$$U_{LJ}(r_{ij}) = 4\epsilon_{ij} \left(\left(\frac{\sigma_{ij}}{r_{ij}} \right)^{12} - \left(\frac{\sigma_{ij}}{r_{ij}} \right)^6 \right) \quad (3.13)$$

Epsilon (ϵ) is the energy well depth and sigma (σ) is the collision diameter where the energy is zero. The U_{LJ} is characterized by a repulsive component that varies as r^{-12} and an attractive component that varies as r^{-6} . The attractive component of the U_{LJ} , models the London or dispersion force that arises from transient dipole-induced dipole interactions [164].

The steep repulsive component is related to the Pauli-exclusion principle [164] stating that when the electron clouds of two atoms come close, they repel each other. Although the value of r^{-12} is not strongly supported theoretically as it produces a too steep repulsive core interaction (an exponential term would be more correct) for many systems including hydrocarbons, it is used by many force fields for large systems for facilitating computational calculations (r^{-12} can be easily calculated by squaring the r^{-6} term). However, some force fields still use values like 9 or 10 for the repulsive component of the U_{LJ} as it provides a less steep curve [141].

For the calculation of 1,4 nonbonded interactions (between atoms that are separated by three bonds) for both the Van der Waals and electrostatic interactions, a different scaling factor (for example 2.0 in the AMBER 1984 force field) is used. This is performed for several reasons, one of them is to reduce the error associated with the use of r^{-12} repulsive term that would be most significant for 1,4 atoms [141].

Coulomb interactions

Difference in electronegativity of elements of a molecule causes an unequal distribution of charge. This uneven charge distribution in a molecule has been represented by different methods with the goal of all of them reproducing the electrostatic properties of the molecule. One of these methods is the central multiple expansion method which treats a molecule as a single entity and is based upon electric moments or multipoles such as dipole, quadrupole and octapole. The other method is the method that works based on assigning dipoles to the bonds in the molecule and then electrostatic energy is obtained

through summing dipole-dipole interaction energies (this is the method used in MM2, MM3 and MM4 force fields). The third method for the representation of uneven charge distribution in a molecule that is the most widely used in MD simulations is the use of partial atomic charges (sometimes also named “net atomic charges”). With the help of the Coulomb’s law, these charges are then used to calculate electrostatic interactions between two molecules as described in equation 3.13 where q_i and q_j are the charges of particles i and j and r_{ij} is the distance between them.

$$U_C(r_{ij}) = f \frac{q_i q_j}{\epsilon_r r_{ij}} \quad (3.14)$$

In this equation, $f = \frac{1}{4\pi\epsilon_0} = 138.935485 \text{ KJ mol}^{-1} \text{ e}^{-2}$ [152] and ϵ_r is a relative dielectric constant.

Since partial atomic charges cannot be unambiguously calculated from the wave function, many different methods have so far been proposed for calculating them. Mulliken charge (that is obtained by population analysis method) and Gasteiger charge (that calculate atomic charges only based on the atoms present in the molecule and their connectivity), are two kinds of charges obtained from these methods however, the electrostatic energy calculated by these methods is not accurate. The third method proposed for calculation of partial atomic charges is using a series of charge points surrounding the molecule to reproduce the QM electrostatic potential. The most famous method is the algorithm Singh and Kollman used in the AMBER 1984 force field that with some modifications was named RESP (restrained electrostatic potential) and introduced for AMBER 1995. In this method, first electrostatic potential at a set of points on the surface of the molecule is calculated from the wave function and then partial atomic charges that best reproduce the electrostatic potential at these points is obtained using a least-squares fitting procedure. The basis set used for deriving the wave function should be carefully selected as a larger basis set does not necessarily improve the results [141].

Although molecular mechanics calculate the energy of the system only as a function of nuclear positions and ignores the electronic motions, however, electronic motions are implicitly considered in the attractive tail of the U_{LJ} and RESP charges. These measures help in considering electronic motions but there is still a big gap for the full representation of electronic motions in molecular mechanics. For example, placing the partial atomic charges on nuclear centers (that assumes spherically symmetrical charge density around each atom) cannot correctly represent the distribution of valence electrons especially in molecules with lone pairs and π electron clouds. The other point is that in normal force fields used in MD simulations, charge distribution within a molecule is considered permanent and therefore the polarization effect induced by the neighboring molecules is ignored [141].

4.2.5 CALCULATING NON-BONDED INTERACTIONS

Calculation of the energies that are related to bonded interactions is not computationally expensive as it is proportional to the number of atoms. This is completely different for non-bonded interactions and the calculation of the energy that is related to non-bonded interactions is considered as the most time-consuming part of an MD simulation. In theory, the non-bonded interactions should be computed between every pair of atoms in the system. To reduce the cost of calculating non-bonded energy, multiple strategies are implemented together while conducting MD simulations including the use of a cut-off radius, calculation of the neighbor lists and Particle mesh Ewald (PME) algorithm for the long range component of the interactions.

Checking all atoms in every time step to see whether they are within the cut off distance value is a computationally heavy task. Therefore, using a procedure called neighbor search, for every particle in the system a neighbor list is provided containing only the atoms within the cutoff distance from that particle. Different algorithms such as Verlet table algorithm and cell linked list algorithm have been used for providing the neighbor list [168] that effectively reduces the burden of calculation of non-bonded interactions. The neighbor list is regularly updated normally every 10 or 20 time steps. The logic behind

this is that neighbors of a particle do not change significantly over 10 or 20 MD time steps [141].

As already mentioned, to calculate the non-bonded interactions as accurately as possible, the PME method is implemented by Gromacs for the calculation of long-range electrostatic and Van der Waals interactions (only the attractive term of the LJ potential) [152]. The electrostatic interactions decay much slower than Van der Waals interactions (as r^{-1}) therefore, truncating electrostatic potential at the cut off distance may lead to severe artifacts [169].

4.2.6 LIMITATIONS OF ALL-ATOM MD SIMULATION FOR THE STUDY OF DDS

For the evaluation of many properties of interest of DDSs, atomistic MD simulations on part of a DDS suffices and will provide us with valuable information. For example, a common approach is to infer results on liposomes from lipid bilayer simulations [140]. However, answering some questions related to the macroscopic properties of a DDS, requires modelling the entire DDS that is generally within a size range of 20–200 nm where possibly tens of millions of atoms should be simulated. In such cases, atomistic MD simulation is not feasible due to the limits in the time and length scales that can be achieved (~15 nm per dimension and microseconds in most cases) [140].

The second limitation in using all atom MD simulation for studying DDSs is related to the fact that the models built often can not predict reliably and precisely some in vivo properties of a DDS; for example the release profile [163]. The reason is that due to the large gap between the molecular and macroscopic scales, predicting the macroscopic properties using simulations with all atom resolution is less realistic [170]. Coarse-grained simulations based on the MARTINI model, can provide a bridge between the atomistic scale and the macroscopic properties of the system [170]. These simulations are commonly used when very large biological systems are to be studied [171-174]. In CG simulations, atoms are grouped into beads to reduce the number of explicit particles thus allowing for an increase in the system size and the simulation time scales by 2–3 orders of magnitude. However, this will lead to

a reduction in the accuracy of the simulation ensemble [143]. There are also some technical complications regarding CG simulations for example reproducing salt and pH effect that should be carefully considered before starting simulations [140]. However, the weakness of CG simulations is the loss of resolution that can be overcome by performing multiscale simulations that take advantage of the best features of each simulation level [147].

5 RESULTS AND DISCUSSION

In this thesis, we conducted all-atom MD simulations on two polymeric and two lipidic drug delivery systems. In each of these studies, a specific property of the DDS was evaluated in detail. For the polymeric DDSs, drug release and size was evaluated and for the liposomes, stability and pH-sensitivity was studied.

5.1 DRUG RELEASE

In study **I**, our experimental colleagues made electrospun loaded biocompatible nanofibrous matrices with polyethylene oxide (PEO) and PCL as polymers and Chloramphenicol (CAM) as the loaded drug. Since PEO and PEG have the same chemical structure and are only different in molecular weight, we refer to the molecule as PEO when discussed in the context of the experimental study, however, since in our computational work we simulated a short segment of this molecule, we referred to it as PEG in this context. They had observed that there is a large difference in the CAM release profile for electrospun mats in the absence and presence of PEO in the polymer composition of polymeric mats (see **Figure 10**). We conducted MD simulations in order to determine how the polymer composition of nanofibers affects the profile of drug release from them. A brief description of the main analysis and results of the study **I**, is presented in **table 1**.

The profile of the drug release is strongly affected by two kinds of interactions; the interactions between drug and the carrier and the interactions between carrier and the surrounding environment. We evaluated these interactions in detail through all atom MD simulations. We determined two reasons for this observation: one the higher hydrophilicity of PEG compared to PCL and the other, stronger interactions between PCL and CAM compared to PCL and PEG. While we had chosen the number of monomers of PEG and PCL in our simulation such that they would have the same number of oxygen atoms, PEG makes much more H-bonds with water in comparison

to PCL indicating the greater hydrophilicity of PEG relative to the case for PCL. Hydrogen bonds that are formed between PEG and water molecules is one of the reasons addition of PEG to PCL, when preparing CAM-loaded electrospun fibers, increases the rate of the drug release. In its structure, CAM has a benzene ring and two chloride groups that cause CAM to form stronger nonpolar–nonpolar contacts with PCL than PEG.

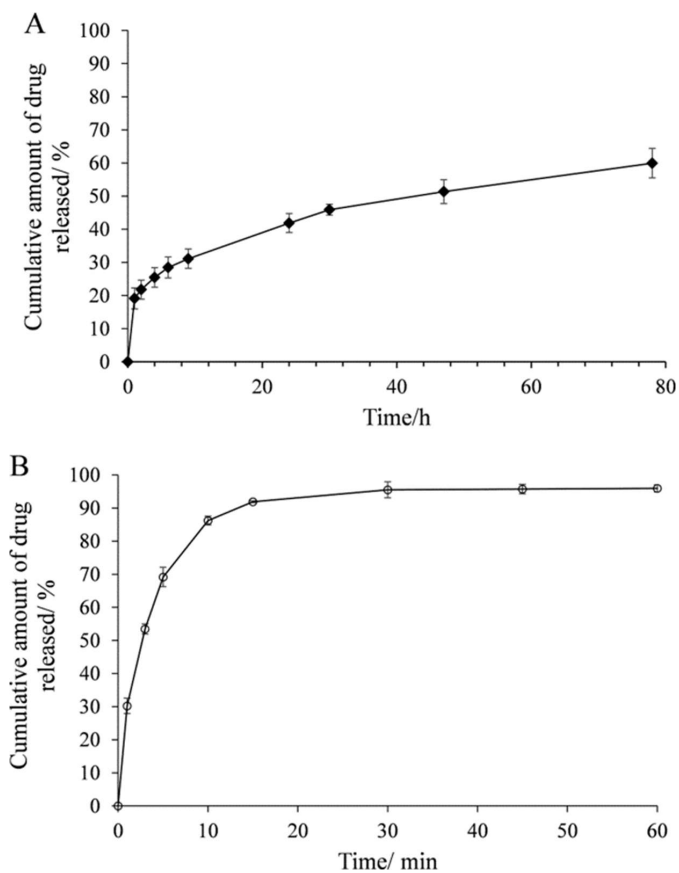


Figure 10. Chloramphenicol release profile from A) drug loaded PCL and B) drug loaded PCL/PEO electrospun nanofiber matrices (from reference [38]). Reprinted with permission from *Mol. Pharmaceutics* 2017, 14, 12, 4417–4430. Copyright 2017 American Chemical Society.

Hydrophobic interactions of PCL and CAM is the driving force in slowing down the release of drug from the fibers as the percentage of PCL to PEG in nanofibers increases. However, one should note that the drug release from a

DDS is a very complicated process that is not only determined by the interactions mentioned above; there are many other driving forces like the initial loaded drug amount that affect the profile of drug release from a DDS.

Table1. A brief description of the main analysis and results of the study I

analysis	model component	result
number of H-bonds formed between polymers and water and between polymers and CAM	PEG in water	Almost twice the number of H-bonds are formed between PEG and water in comparison to the case for PCL and water. Few H-bonds are formed between polymers and CAM
	PCL in water	
% polar and non-polar surface area of CAM in contact with PEG and PCL	CAM and PEG in water	During almost all the simulation time, PCL has been in contact with both polar and non polar surface of CAM. This amount is much less for PEG
	CAM and PCL in water	
Radius of gyration	PEG in water	radius of gyration of PCL and PEG did not significantly change in the presence of CAM. Thus, polymers remained linear in the course of simulation
	PCL in water	
	PEG and CAM in water	
	PEG and PCL in water	
Evaluation of different types of contacts between polymers and CAM	PEG and CAM	nonpolar–nonpolar interactions are the dominant form of interaction between CAM and PCL and CAM and PEG. From the total contacts between polymers and CAM, polar–polar contacts contribute only to a very small extent.
	PCL and CAM	

5.2 STABILITY

Rapid clearance of nanoparticles from the blood stream could be prevented through surface modification of nanoparticles. The large surface area of the nanoparticles provides the possibility for surface modification as mentioned previously, the gold standard of which is PEGylation. To stabilize liposomes in the blood stream and to increase their blood circulation time, PEG as a protective polymer is attached to the surface of liposomes. In study **II**, we evaluated how PEG length (2 kDa and 5 kDa), shape (linear and branched PEG) and its anchoring moiety (DSPE, Chol, Cholane (Chln)) may affect the stability of liposomes. A brief description of the main analysis and results of the study **II** is presented in **table 2**.

The results of our simulations, especially the evaluation of orientation of Chln in the bilayer, led us to the conclusion that liposomes containing PEG with Chln as the anchoring moiety have the lowest stability, in line with the results our experimental colleagues obtained. However, determining which liposomes have the highest stability through computational simulations is a much more complicated issue. Even our experimental colleagues obtained different results regarding the most stable liposome in vitro and in vivo. While in vitro experimental results demonstrated that branched PEG anchored to liposomes through DSPE has the highest stability, in vivo results demonstrated that liposomes with Chol as the anchoring agent are the most stable. In MD simulations, we make a model of the system where it is simplified as much as possible to prevent complicated interactions and to reduce computational cost but still be able to elucidate the phenomena we investigate; the result is a difficult balance and important phenomena can be left out. Therefore, as it was discussed in the introduction section, one should be careful not to over interpret computational results as even in vitro and in vivo results would be different regarding multi factorial dependent properties of nanoparticles like stability.

Table2. A brief description of the main analysis and results of the study II

analysis	model component	result
mass density profile of PEG		Compared to the systems with shorter PEG length (mPEG45), the systems with PEG coating layer of mPEG114 and branched (mPEG114) ₂ demonstrated considerably thicker PEG coating on the surface. Among different systems, the one with branched PEG exhibited a greater density further from the membrane surface.
electrostatic potential	In this publication, we conducted MD simulations on six models. All of the analysis were conducted on all of these six models that are:	The electrostatic potential change from the center of the bilayer to the surface of the membrane is lower for the system PEGylated with mPEG114-Chln than with other PEGylating agents indicating a looser, less ordered membrane structure
Deuterium order parameter	PEG45-DSPE, DSPC, Chol PEG114-DSPE, DSPC, Chol PEG45-Chol, DSPC, Chol PEG114-Chol, DSPC, Chol PEG45-Chln, DSPC, Chol PEG114-Chln, DSPC, Chol (PEG114) ₂ -DSPE, DSPC, Chol	The lowest extent of lipid tail order belongs to the system with mPEG114-Chln as the PEGylating agent. This, once again, indicates a decreased lipid order.
Orientation of Chln in the Membrane		We observed that when Chln is attached to PEG, it orients in the membrane in an inverted orientation with respect to the Chol. When Chln is not attached to PEG, there is no preferred orientation for Chln within the membrane core.

5.3 PH-SENSITIVITY

In the study **III**, we conducted MD simulations on pH-sensitive liposomes composed of DOPE and CHMS to determine the mechanisms behind the stabilization and destabilization of these liposomes upon pH change. A brief description of the main analysis and results of the study **III** is presented in table 3.

Three mechanisms have already been proposed regarding how CHSa (CHMS in its anionic form in neutral pH) stabilize pH-sensitive liposomes that are: disruption of the intermolecular interaction between adjacent PEs [175], increasing liposomal interfacial hydration [128] and the electrostatic repulsion provided by CHSa [131]. Based on our results, CHSa does not stabilize DOPE bilayers through decreasing intermolecular H-bonds as we did not observe a reduction in the number of inter-lipid H-bonds in DOPE-CHSa in comparison to DOPE-CHOL. We also determined that CHSa does not stabilize pH-sensitive liposomes through providing electrostatic repulsion. Our observations were in line with the results Klasczyk et al [176] obtained that CHSa adsorbs all cations in the simulation excluding the theory of electrostatic stabilization of charged bilayers.

The low hydration extent of DOPE, is the reason for the high tendency of DOPE bilayers to undergo a lamellar-to-hexagonal phase transition [128]. Following our MD simulations, we came to this conclusion that CHSa stabilizes the DOPE lipid membrane by increasing the hydrophilicity of the bilayer surface through forming a high number of H-bonds with water molecules.

Destabilization of pH-sensitive DOPE-CHMS liposomes is triggered with a reduction in pH and the change of CHSa to CHS (CHMS in its protonated form in acidic pH). Following this change, the bilayer surface is dehydrated and the number of bonded Na^+ ions to the lipid head groups is reduced. Therefore, the area per molecule reduces and based on dynamic molecular shape theory applied to lipids [177], the cone shaped DOPE lipids undergo a phase transition from lamellar to hexagonal II (see **Figure 11**).

Table3. A brief description of the main analysis and results of the study III

analysis	model components	results
Area per molecule	<p>In this publication, We conducted MD simulations on six models. All of the analysis were conducted on all of these six models that are:</p> <p>DOPE-CHOL DOPE-CHS DOPE-CHSa PEG-DOPE-CHOL PEG-DOPE-CHS PEG-DOPE-CHSa</p>	Among non PEGylated systems, DOPE-CHSa has the lowest area per lipid. We observed that PEGylation increases surface area. We also observed a reduction in area per molecule as CHSa changes to CHS
Membrane hydration		Based on water mass density profile, bilayers with CHOL show the deepest water penetration into the bilayer and also with PEGylation, a reduction in the amount of water penetration is observed. Bilayers with CHS have the lowest number of bilayer-water contacts and bilayer-water H-bonds.
deuterium order parameter		The lowest deuterium order parameter among non PEGylated systems belongs to DOPE-CHSa. For all the systems, PEGylation reduced the order parameter.
Ion contacts with bilayer and PEG		We observed that the strongest bilayer- Na^+ binding occurs in systems containing CHSa that are DOPE-CHSa and PEG-DOPE-CHSa. When systems are PEGylated, the percentage of Na^+ ions in contact with the bilayer decreases.
PEG Penetration into the Lipid Bilayers		PEG penetrates into lipid bilayers and the lowest amount of PEG penetration into the bilayer is found for the PEG-DOPE-CHSa system.


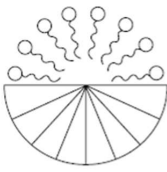
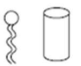
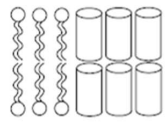

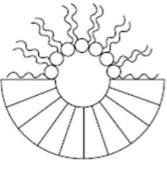
Species	Shape	Organization	Phase
Soaps Detergents Lysophospholipids	 Inverted cone	 Micelles	Isotropic Hexagonal 1
Phosphatidylcholine Phosphatidylserine Phosphatidylinositol Sphingomyelin Dicetylphosphate DODAC	 Cylinder	 Bilayer	Lamellar (Cubic)
Phosphatidylethanolamine Phosphatidic acid Cholesterol Cardiolipin Lipid A	 Cone	 Reverse micelles	Hexagonal 2

Figure 11. The effect of molecular shape on the structure of the amphiphilic aggregate. Reprinted from [97] with permission from Elsevier.

It is worth mentioning that to reduce computational cost and scientific complexities, in this study, only one bilayer exists in each simulation box where DOPE is fully hydrated. In the experimental condition, there are thousands of liposomes in the solution that will encounter the occurrence of a narrow fluid space phenomena, inter bilayer contact and a strong adherence between opposing PE bilayers from the neighboring liposomes (originates from electrostatic interactions between the NH_3^+ group in one bilayer and the PO_4^- group in the opposing bilayers) [178]. Therefore, beside what we determined regarding the mechanisms of stabilization and destabilization of pH-sensitive liposomes, it is recommended that these mechanisms also be evaluated in multi bilayer models.

To increase the blood circulation time of the pH-sensitive liposomes, they are decorated with PEG however, it is experimentally proved that the use of PEG will dramatically reduce the pH-sensitivity of pH-sensitive liposomes [121, 122]. In part of study **III**, we attempted to determine how PEG stabilizes pH-sensitive liposomes composed of DOPE and CHMS in the lamellar phase and prevents the lamellar to hexagonal phase transition and consequently reduces the pH-sensitivity of pH-sensitive liposomes.

PEG stabilizes liposomes using different mechanisms one of which is providing a steric hindrance around the liposomes inhibiting the approach of other liposomes [179, 180]. This steric hindrance, will prevent inter bilayer contact of liposomes that is necessary for the process of phase transition to start [181]. This mechanism seems to work more in in vitro condition than in in vivo condition. The other mechanism as discussed in the section 2.2.1 is related to helping nanoparticles to evade the MPS. However, for the DOPE lipid bilayers, through our MD simulation, we found another mechanism for the stabilizing effect of PEG: it significantly penetrates into the lipid bilayer and increases the area per molecule that based on dynamic molecular shape concept for the lipids, prevents the phase transition of the DOPE bilayers from lamellar to hexagonal. On the other hand, PE-PEG is an inverted cone shaped lipid derivative that is experimentally proved to stabilize a mixture of cone shaped lipids (DOPE and Chol) in the lamellar conformation [180].

5.4 SIZE

As mentioned in section 2.1.2, polymeric nanoparticles may be formed by different methods with the self-assembly of polymeric chains as the most common. Depending on the chemical structure of the polymeric chains that are going to be formed into nanoparticles, the method of self-assembly of polymeric chains would be different and, as a result, particles with different sizes will be formed. Size of the nanoparticles is crucial for their success as it affects their physicochemical, pharmaceutical and biological properties [182]. In study **IV**, our experimental colleagues made nanoparticles through self-assembly of chitosan (CS) and phosphate glucan (PG) polymeric chains by

using the ion gelation method. They observed that with increasing temperature in the process of nanoparticle formation, smaller polymeric particles are formed. They requested us to conduct MD simulations to determine how smaller particles are formed upon increase in temperature in the process of particle formation.

Through conducting MD simulations on a system composed of ten CS chains (each containing six monomers with a plus four charge) and twenty PG chains (each containing six monomers with minus two charge) in different temperatures, we attempted to determine the mechanism through which increasing temperature would lead to the formation of smaller polymeric nanoparticles. A brief description of the main analysis and results of the study **IV** is presented in **table4**.

We observed that with increasing temperature, the number of H-bonds between both PG and CS with water decreases and the number of contacts and H-bonds between CS and PG chains increases. This would lead to significantly higher interactions among polymeric chains however, the process of particle formation is extremely complex and it is very difficult to determine how these higher interactions would lead to formation of smaller particles. This complexity in the mechanism of formation of CS/PG particles is observed in the experimental data our colleagues obtained. They used bulk method and different microfluidic methods for the formation of CS/PG particles each leading to the formation of particles with a different size even when all other experimental parameters including temperature were the same. When our experimental colleagues used the bulk method for the formation of CS/PG particles, particles with the size of 257 ± 34 nm were formed in room temperature and then at 65°C , particles with a size of 212 ± 25 nm were formed as measured by dynamic light scattering. When CS/PG particles were formed using a microfluidic chip method, at room temperature particles with a size of 182 ± 9 nm were formed and when the temperature increased to 65°C , the size of the NPs was remarkably reduced to 102 ± 10 nm.

Table4. A brief description of the main analysis and results of the study **IV**

Analysis	model components	results
radius of gyration	Ten CS and twenty PG chains	In all the three temperatures, the radius of gyration of CS is greater than PG. However, the radius of gyration of both CS and PG remained constant as the temperature increased
inter polymer contacts		At all three temperatures investigated, the number of contacts between PG chains is almost twice the number of contacts between CS chains. The number of contacts between CS and PG chains increases as the temperature increases
polymer-water contacts		At all three temperatures investigated, the number of PG-water contacts is almost three times the number of CS-water contacts. With the increase in temperature, the number of contacts between both PG and CS and water decreases.
number of H-bonds		With increasing temperature, the number of H-bonds between both CS and PG with water reduces and the number of H-bonds between CS and PG chains increases.
number of polymer clusters		With increasing temperature, the number of formed polymeric clusters increases thus, smaller polymeric particles are formed.

Although MD simulations help to shed light on the mechanism of formation of smaller CS/PG nanoparticles upon increase in the temperature, however, the process of particle formation is controlled by many factors not all of them could be evaluated by MD simulations. For example, it is not possible to differentiate between bulk and micro fluidic methods by MD simulations. On the other hand, to reduce the computational cost, we had to simulate polymeric chains with a significantly shorter length in comparison to what was used in experiments that makes it more difficult to determine the mechanisms behind particle formation. As it is stated in table 4, the radius of gyration of both CS and PG remained constant upon increase in temperature that could be an artifact of their short length.

6 CONCLUSIONS

Drug delivery systems are mainly used 1- to decrease severe dose limiting side effects and unsatisfactory therapeutic results of drugs in particular anti-cancer agents following systemic administration 2- to improve the pharmacokinetic properties of drugs. Drug delivery systems now have proved their ability in decreasing the side effects of drugs while also improving drug bioavailability and pharmacokinetics.

An ideal DDS should have many characteristics including long blood circulation time, high accumulation in target tissue and a controlled release profile. A DDS optimized for these characteristics could hardly be obtained using only experimental investigation. In the process of developing and optimizing DDSs, often questions arise that are difficult to address experimentally especially when it is necessary to know the specific interactions between different components of a DDS and when mechanisms behind an experimental observation need to be elucidated.

In this thesis, we conducted all-atom MD simulations on two polymeric and two lipidic DDSs to obtain an accurate picture of the interactions and mechanisms that govern drug release profile (study **I**), stability (study **II**), pH-sensitivity (study **III**) and size (study **IV**) of DDSs. As it was discussed in detail in the discussion section, through conducting MD simulations we managed to shed light on the mechanisms that led to experimental results and determined that the MD simulation has the capacity to complement the experimental development and optimization of DDSs through providing insight that is difficult or impossible to obtain experimentally. However, one should be careful not to be misled by artifacts and limitations of MD simulations and not to misinterpret while making a comparison between simulations and experiment results.

7 REFERENCES

1. Dong P, Rakesh K, Manukumar H, Mohammed YHE, Karthik C, Sumathi S, Mallu P, Qin H-L. Innovative nano-carriers in anticancer drug delivery-a comprehensive review. *Bioorganic chemistry*. 2019;85:325-36.
2. Olusanya TO, Haj Ahmad RR, Ibegbu DM, Smith JR, Elkordy AA. Liposomal drug delivery systems and anticancer drugs. *Molecules*. 2018;23(4):907.
3. Xin Y, Yin M, Zhao L, Meng F, Luo L. Recent progress on nanoparticle-based drug delivery systems for cancer therapy. *Cancer biology & medicine*. 2017;14(3):228.
4. Danesi R, Fogli S, Gennari A, Conte P, Del Tacca M. Pharmacokinetic-pharmacodynamic relationships of the anthracycline anticancer drugs. *Clinical pharmacokinetics*. 2002;41(6):431-44.
5. Suter TM, Ewer MS. Cancer drugs and the heart: importance and management. *European heart journal*. 2013;34(15):1102-11.
6. Sereno M, Brunello A, Chiappori A, Barriuso J, Casado E, Belda C, de Castro J, Feliu J, Gonzalez-Baron M. Cardiac toxicity: old and new issues in anti-cancer drugs. *Clinical and Translational Oncology*. 2008;10(1):35-46.
7. Mazzaferro S, Bouchemal K, Ponchel G. Oral delivery of anticancer drugs I: general considerations. *Drug discovery today*. 2013;18(1-2):25-34.
8. Ailincai D, Tartau Mititelu L, Marin L. Drug delivery systems based on biocompatible imino-chitosan hydrogels for local anticancer therapy. *Drug delivery*. 2018;25(1):1080-90.
9. Wang Y, Wang J, Yuan Z, Han H, Li T, Li L, Guo X. Chitosan cross-linked poly (acrylic acid) hydrogels: drug release control and mechanism. *Colloids and Surfaces B: Biointerfaces*. 2017;152:252-9.
10. Zhao J, Cui W. Functional electrospun fibers for local therapy of cancer. *Advanced Fiber Materials*. 2020:1-17.
11. Cavo M, Serio F, Kale NR, D'Amone E, Gigli G, Loretta L. Electrospun nanofibers in cancer research: from engineering of in vitro 3D cancer models to therapy. *Biomaterials Science*. 2020;8(18):4887-905.
12. Sung YK, Kim SW. Recent advances in polymeric drug delivery systems. *Biomaterials Research*. 2020;24(1):1-12.
13. Naskar S, Kuotsu K, Sharma S. Chitosan-based nanoparticles as drug delivery systems: a review on two decades of research. *Journal of drug targeting*. 2019;27(4):379-93.
14. Huang G, Huang H. Application of dextran as nanoscale drug carriers. *Nanomedicine*. 2018;13(24):3149-58.
15. Klose D, Siepmann F, Elkharraz K, Siepmann J. PLGA-based drug delivery systems: importance of the type of drug and device geometry. *International journal of pharmaceutics*. 2008;354(1-2):95-103.
16. Avramović N, Mandić B, Savić-Radojević A, Simić T. Polymeric nanocarriers of drug delivery systems in cancer therapy. *Pharmaceutics*. 2020;12(4):298.
17. Li M, Du C, Guo N, Teng Y, Meng X, Sun H, Li S, Yu P, Galons H. Composition design and medical application of liposomes. *European journal of medicinal chemistry*. 2019;164:640-53.
18. Karanth H, Murthy R. pH-Sensitive liposomes-principle and application in cancer therapy. *Journal of pharmacy and pharmacology*. 2007;59(4):469-83.

19. Zhang C, Ding Y, Yu LL, Ping Q. Polymeric micelle systems of hydroxycamptothecin based on amphiphilic N-alkyl-N-trimethyl chitosan derivatives. *Colloids and Surfaces B: Biointerfaces*. 2007;55(2):192-9.
20. Xiangyang X, Ling L, Jianping Z, Shiyue L, Jie Y, Xiaojin Y, Jinsheng R. Preparation and characterization of N-succinyl-N'-octyl chitosan micelles as doxorubicin carriers for effective anti-tumor activity. *Colloids and Surfaces B: Biointerfaces*. 2007;55(2):222-8.
21. Lao S-B, Zhang Z-X, Xu H-H, Jiang G-B. Novel amphiphilic chitosan derivatives: synthesis, characterization and micellar solubilization of rotenone. *Carbohydrate Polymers*. 2010;82(4):1136-42.
22. Balusamy B, Celebioglu A, Senthamizhan A, Uyar T. Progress in the design and development of "fast-dissolving" electrospun nanofibers based drug delivery systems-A systematic review. *Journal of Controlled Release*. 2020.
23. Kajdič S, Planinšek O, Gašperlin M, Kocbek P. Electrospun nanofibers for customized drug-delivery systems. *Journal of Drug Delivery Science and Technology*. 2019;51:672-81.
24. Schwinté P, Mariotte A, Anand P, Keller L, Idoux-Gillet Y, Huck O, Fioretti F, Tenenbaum H, Georgel P, Wenzel W. Anti-inflammatory effect of active nanofibrous polymeric membrane bearing nanocontainers of atorvastatin complexes. *Nanomedicine*. 2017;12(23):2651-74.
25. Yu D-G, Zhu L-M, White K, Branford-White C. Electrospun nanofiber-based drug delivery systems. *Health*. 2009;1(02):67.
26. Wsoo MA, Shahir S, Bohari SPM, Nayan NHM, Abd Razak SI. A review on the properties of electrospun cellulose acetate and its application in drug delivery systems: A new perspective. *Carbohydrate research*. 2020;491:107978.
27. Ghafoor B, Aleem A, Ali MN, Mir M. Review of the fabrication techniques and applications of polymeric electrospun nanofibers for drug delivery systems. *Journal of Drug Delivery Science and Technology*. 2018;48:82-7.
28. Radisavljevic A, Stojanovic DB, Perisic S, Djokic V, Radojevic V, Rajilic-Stojanovic M, Uskokovic PS. Cefazolin-loaded polycaprolactone fibers produced via different electrospinning methods: Characterization, drug release and antibacterial effect. *European Journal of Pharmaceutical Sciences*. 2018;124:26-36.
29. Celebioglu A, Uyar T. Electrospun formulation of acyclovir/cyclodextrin nanofibers for fast-dissolving antiviral drug delivery. *Materials Science and Engineering: C*. 2021;118:111514.
30. Tuğcu-Demiröz F, Saar S, Tort S, Acartürk F. Electrospun metronidazole-loaded nanofibers for vaginal drug delivery. *Drug Development and Industrial Pharmacy*. 2020;46(6):1015-25.
31. Eskitoros-Togay ŞM, Bulbul YE, Tort S, Korkmaz FD, Acartürk F, Dilsiz N. Fabrication of doxycycline-loaded electrospun PCL/PEO membranes for a potential drug delivery system. *International journal of pharmaceutics*. 2019;565:83-94.
32. Grant JJ, Pillai SC, Perova TS, Hehir S, Hinder SJ, McAfee M, Breen A. Electrospun fibres of chitosan/PVP for the effective chemotherapeutic drug delivery of 5-fluorouracil. *Chemosensors*. 2021;9(4):70.
33. Wu J, Zhang Z, Zhou W, Liang X, Zhou G, Han CC, Xu S, Liu Y. Mechanism of a long-term controlled drug release system based on simple blended electrospun fibers. *Journal of Controlled Release*. 2020;320:337-46.
34. Zeng J, Yang L, Liang Q, Zhang X, Guan H, Xu X, Chen X, Jing X. Influence of the drug compatibility with polymer solution on the release

- kinetics of electrospun fiber formulation. *Journal of controlled release*. 2005;105(1-2):43-51.
35. Aytac Z, Ipek S, Erol I, Durgun E, Uyar T. Fast-dissolving electrospun gelatin nanofibers encapsulating ciprofloxacin/cyclodextrin inclusion complex. *Colloids and Surfaces B: Biointerfaces*. 2019;178:129-36.
 36. Wang Y, Deng Z, Wang X, Shi Y, Lu Y, Fang S, Liang X. Formononetin/methyl- β -cyclodextrin inclusion complex incorporated into electrospun polyvinyl-alcohol nanofibers: Enhanced water solubility and oral fast-dissolving property. *International Journal of Pharmaceutics*. 2021;603:120696.
 37. Steffens L, Morás AM, Arantes PR, Masterson K, Cao Z, Nugent M, Moura DJ. Electrospun PVA-Dacarbazine nanofibers as a novel nano brain-implant for treatment of glioblastoma: in silico and in vitro characterization. *European Journal of Pharmaceutical Sciences*. 2020;143:105183.
 38. Preem L, Mahmoudzadeh M, Putrinš M, Meos A, Laidmäe I, Romann T, Aruväli J, Härmas R, Koivuniemi A, Bunker A. Interactions between chloramphenicol, carrier polymers, and bacteria—implications for designing electrospun drug delivery systems countering wound infection. *Molecular pharmaceutics*. 2017;14(12):4417-30.
 39. Li J, Mooney DJ. Designing hydrogels for controlled drug delivery. *Nature Reviews Materials*. 2016;1(12):1-17.
 40. Vigata M, Meinert C, Hutmacher DW, Bock N. Hydrogels as drug delivery systems: A review of current characterization and evaluation techniques. *Pharmaceutics*. 2020;12(12):1188.
 41. Ullah F, Othman MBH, Javed F, Ahmad Z, Akil HM. Classification, processing and application of hydrogels: A review. *Materials Science and Engineering: C*. 2015;57:414-33.
 42. Ito T, Takami T, Uchida Y, Murakami Y. Chitosan gel sheet containing drug carriers with controllable drug-release properties. *Colloids and Surfaces B: Biointerfaces*. 2018;163:257-65.
 43. McKenzie M, Betts D, Suh A, Bui K, Kim LD, Cho H. Hydrogel-based drug delivery systems for poorly water-soluble drugs. *Molecules*. 2015;20(11):20397-408.
 44. Vashist A, Vashist A, Gupta Y, Ahmad S. Recent advances in hydrogel based drug delivery systems for the human body. *Journal of Materials Chemistry B*. 2014;2(2):147-66.
 45. Kirchmayer DM, Gorkin Iii R. An overview of the suitability of hydrogel-forming polymers for extrusion-based 3D-printing. *Journal of Materials Chemistry B*. 2015;3(20):4105-17.
 46. Norouzi M, Nazari B, Miller DW. Injectable hydrogel-based drug delivery systems for local cancer therapy. *Drug discovery today*. 2016;21(11):1835-49.
 47. An M, Demir B, Wan X, Meng H, Yang N, Walsh TR. Predictions of Thermo-Mechanical Properties of Cross-Linked Polyacrylamide Hydrogels Using Molecular Simulations. *Advanced Theory and Simulations*. 2019;2(3):1800153.
 48. Sun D, Zhou J. Effect of water content on microstructures and oxygen permeation in PSiMA-IPN-PMPC hydrogel: a molecular simulation study. *Chemical engineering science*. 2012;78:236-45.
 49. Jiang X, Wang C, Han Q. Molecular dynamic simulation on the state of water in poly (vinyl alcohol) hydrogel. *Computational and Theoretical Chemistry*. 2017;1102:15-21.
 50. Pascal TA, He Y, Jiang S, Goddard III WA. Thermodynamics of water stabilization of carboxybetaine hydrogels from molecular dynamics simulations. *The Journal of Physical Chemistry Letters*. 2011;2(14):1757-60.

51. He Y, Tsao H-K, Jiang S. Improved mechanical properties of zwitterionic hydrogels with hydroxyl groups. *The Journal of Physical Chemistry B*. 2012;116(19):5766-70.
52. Erbas A, Olvera de la Cruz M. Energy conversion in polyelectrolyte hydrogels. *ACS Macro Letters*. 2015;4(8):857-61.
53. Mathesan S, Rath A, Ghosh P. Molecular mechanisms in deformation of cross-linked hydrogel nanocomposite. *Materials Science and Engineering: C*. 2016;59:157-67.
54. Yan C, Kramer PL, Yuan R, Fayer MD. Water dynamics in polyacrylamide hydrogels. *Journal of the American Chemical Society*. 2018;140(30):9466-77.
55. Vauthier C, Bouchemal K. Methods for the preparation and manufacture of polymeric nanoparticles. *Pharmaceutical research*. 2009;26(5):1025-58.
56. Zielińska A, Carreiró F, Oliveira AM, Neves A, Pires B, Venkatesh DN, Durazzo A, Lucarini M, Eder P, Silva AM. Polymeric nanoparticles: production, characterization, toxicology and ecotoxicology. *Molecules*. 2020;25(16):3731.
57. Soppimath KS, Aminabhavi TM, Kulkarni AR, Rudzinski WE. Biodegradable polymeric nanoparticles as drug delivery devices. *Journal of controlled release*. 2001;70(1-2):1-20.
58. Kumari A, Yadav SK, Yadav SC. Biodegradable polymeric nanoparticles based drug delivery systems. *Colloids and surfaces B: biointerfaces*. 2010;75(1):1-18.
59. Crucho CI, Barros MT. Polymeric nanoparticles: A study on the preparation variables and characterization methods. *Materials Science and Engineering: C*. 2017;80:771-84.
60. Rao JP, Geckeler KE. Polymer nanoparticles: preparation techniques and size-control parameters. *Progress in polymer science*. 2011;36(7):887-913.
61. Corrigan OI, Li X. Quantifying drug release from PLGA nanoparticulates. *European Journal of Pharmaceutical Sciences*. 2009;37(3-4):477-85.
62. Park K, Kim J-H, Nam YS, Lee S, Nam HY, Kim K, Park JH, Kim I-S, Choi K, Kim SY. Effect of polymer molecular weight on the tumor targeting characteristics of self-assembled glycol chitosan nanoparticles. *Journal of Controlled Release*. 2007;122(3):305-14.
63. Jiang G-B, Quan D, Liao K, Wang H. Preparation of polymeric micelles based on chitosan bearing a small amount of highly hydrophobic groups. *Carbohydrate Polymers*. 2006;66(4):514-20.
64. Yang X, Zhang Q, Wang Y, Chen H, Zhang H, Gao F, Liu L. Self-aggregated nanoparticles from methoxy poly (ethylene glycol)-modified chitosan: synthesis; characterization; aggregation and methotrexate release in vitro. *Colloids and Surfaces B: Biointerfaces*. 2008;61(2):125-31.
65. Gaucher G, Dufresne M-H, Sant VP, Kang N, Maysinger D, Leroux J-C. Block copolymer micelles: preparation, characterization and application in drug delivery. *Journal of controlled release*. 2005;109(1-3):169-88.
66. Kwon GS, Forrest ML. Amphiphilic block copolymer micelles for nanoscale drug delivery. *Drug development research*. 2006;67(1):15-22.
67. Houdaihed L, Evans JC, Allen C. Overcoming the road blocks: advancement of block copolymer micelles for cancer therapy in the clinic. *Molecular pharmaceuticals*. 2017;14(8):2503-17.
68. Ciro Y, Rojas J, Oñate-Garzon J, Salamanca CH. Synthesis, characterisation and biological evaluation of ampicillin–chitosan–polyanion nanoparticles produced by ionic gelation and polyelectrolyte complexation assisted by high-intensity sonication. *Polymers*. 2019;11(11):1758.

69. Hamman JH. Chitosan based polyelectrolyte complexes as potential carrier materials in drug delivery systems. *Marine drugs*. 2010;8(4):1305-22.
70. Matsumura Y, Maeda H. A new concept for macromolecular therapeutics in cancer chemotherapy: mechanism of tumoritropic accumulation of proteins and the antitumor agent smancs. *Cancer research*. 1986;46(12 Part 1):6387-92.
71. Maeda H. Tumor-selective delivery of macromolecular drugs via the EPR effect: background and future prospects. *Bioconjugate chemistry*. 2010;21(5):797-802.
72. Noguchi Y, Wu J, Duncan R, Strohalm J, Ulbrich K, Akaike T, Maeda H. Early phase tumor accumulation of macromolecules: a great difference in clearance rate between tumor and normal tissues. *Japanese Journal of Cancer Research*. 1998;89(3):307-14.
73. Fang J, Nakamura H, Maeda H. The EPR effect: unique features of tumor blood vessels for drug delivery, factors involved, and limitations and augmentation of the effect. *Advanced drug delivery reviews*. 2011;63(3):136-51.
74. Maeda H. Toward a full understanding of the EPR effect in primary and metastatic tumors as well as issues related to its heterogeneity. *Advanced drug delivery reviews*. 2015;91:3-6.
75. Shi Y, Van der Meel R, Chen X, Lammers T. The EPR effect and beyond: Strategies to improve tumor targeting and cancer nanomedicine treatment efficacy. *Theranostics*. 2020;10(17):7921.
76. Maeda H, Wu J, Sawa T, Matsumura Y, Hori K. Tumor vascular permeability and the EPR effect in macromolecular therapeutics: a review. *Journal of controlled release*. 2000;65(1-2):271-84.
77. Wilhelm S, Tavares AJ, Dai Q, Ohta S, Audet J, Dvorak HF, Chan WC. Analysis of nanoparticle delivery to tumours. *Nature reviews materials*. 2016;1(5):1-12.
78. Maeda H. The 35th Anniversary of the Discovery of EPR Effect: A New Wave of Nanomedicines for Tumor-Targeted Drug Delivery—Personal Remarks and Future Prospects. *Journal of personalized medicine*. 2021;11(3):229.
79. Fang J, Islam W, Maeda H. Exploiting the dynamics of the EPR effect and strategies to improve the therapeutic effects of nanomedicines by using EPR effect enhancers. *Advanced drug delivery reviews*. 2020;157:142-60.
80. Kang H, Rho S, Stiles WR, Hu S, Baek Y, Hwang DW, Kashiwagi S, Kim MS, Choi HS. Size-dependent EPR effect of polymeric nanoparticles on tumor targeting. *Advanced healthcare materials*. 2020;9(1):1901223.
81. Liu Z, Lian W, Long Q, Cheng R, Torrieri G, Zhang B, Koivuniemi A, Mahmoudzadeh M, Bunker A, Gao H. Promoting Cardiac Repair through Simple Engineering of Nanoparticles with Exclusive Targeting Capability toward Myocardial Reperfusion Injury by Thermal Resistant Microfluidic Platform. *Advanced Functional Materials*. 2022;32(36):2204666.
82. Rezaeisadat M, Bordbar A-K, Omidyan R. Molecular dynamics simulation study of curcumin interaction with nano-micelle of PNIPAAm-b-PEG co-polymer as a smart efficient drug delivery system. *Journal of Molecular Liquids*. 2021;332:115862.
83. Li J, Ying S, Ren H, Dai J, Zhang L, Liang L, Wang Q, Shen Q, Shen J-W. Molecular dynamics study on the encapsulation and release of anti-cancer drug doxorubicin by chitosan. *International Journal of Pharmaceutics*. 2020;580:119241.
84. Wilkosz N, Łazarski G, Kovacic L, Gargas P, Nowakowska M, Jamróz D, Kepczynski M. Molecular insight into drug-loading capacity of

- PEG–PLGA nanoparticles for itraconazole. *The Journal of Physical Chemistry B*. 2018;122(28):7080-90.
85. Samanta S, Roccatano D. Interaction of curcumin with PEO–PPO–PEO block copolymers: a molecular dynamics study. *The Journal of Physical Chemistry B*. 2013;117(11):3250-7.
86. He J, Chipot C, Shao X, Cai W. Cyclodextrin-mediated recruitment and delivery of amphotericin B. *The Journal of Physical Chemistry C*. 2013;117(22):11750-6.
87. Shan P, Shen J-W, Xu D-H, Shi L-Y, Gao J, Lan Y-W, Wang Q, Wei X-H. Molecular dynamics study on the interaction between doxorubicin and hydrophobically modified chitosan oligosaccharide. *Rsc Advances*. 2014;4(45):23730-9.
88. Li C, Tho CC, Galaktionova D, Chen X, Král P, Mirsaidov U. Dynamics of amphiphilic block copolymers in an aqueous solution: direct imaging of micelle formation and nanoparticle encapsulation. *Nanoscale*. 2019;11(5):2299-305.
89. Mahmoudzadeh M, Fassihi A, Dorkoosh F, Heshmatnejad R, Mahnam K, Sabzyan H, Sadeghi A. Elucidation of molecular mechanisms behind the self-assembly behavior of chitosan amphiphilic derivatives through experiment and molecular modeling. *Pharmaceutical research*. 2015;32(12):3899-915.
90. Zhang C, Liu T, Wang W, Bell CA, Han Y, Fu C, Peng H, Tan X, Král P, Gaus K. Tuning of the aggregation behavior of fluorinated polymeric nanoparticles for improved therapeutic efficacy. *ACS nano*. 2020;14(6):7425-34.
91. Van Lehn RC, Alexander-Katz A. Pathway for insertion of amphiphilic nanoparticles into defect-free lipid bilayers from atomistic molecular dynamics simulations. *Soft Matter*. 2015;11(16):3165-75.
92. Van Lehn RC, Ricci M, Silva PH, Andreozzi P, Reguera J, Voitchovsky K, Stellacci F, Alexander-Katz A. Lipid tail protrusions mediate the insertion of nanoparticles into model cell membranes. *Nature communications*. 2014;5(1):1-11.
93. Crommelin DJ, van Hoogevest P, Storm G. The role of liposomes in clinical nanomedicine development. What now? Now what? *Journal of Controlled Release*. 2020;318:256-63.
94. Trucillo P, Campardelli R, Reverchon E. Liposomes: From bangham to supercritical fluids. *Processes*. 2020;8(9):1022.
95. Guimarães D, Cavaco-Paulo A, Nogueira E. Design of liposomes as drug delivery system for therapeutic applications. *International Journal of Pharmaceutics*. 2021;601:120571.
96. Rideau E, Dimova R, Schwille P, Wurm FR, Landfester K. Liposomes and polymersomes: a comparative review towards cell mimicking. *Chemical society reviews*. 2018;47(23):8572-610.
97. Lasic DD. Novel applications of liposomes. *Trends in biotechnology*. 1998;16(7):307-21.
98. Bozzuto G, Molinari A. Liposomes as nanomedical devices. *International journal of nanomedicine*. 2015;10:975.
99. Mastrotto F, Brazzale C, Bellato F, De Martin S, Grange G, Mahmoudzadeh M, Magarkar A, Bunker A, Salmasso S, Caliceti P. In vitro and in vivo behavior of liposomes decorated with PEGs with different chemical features. *Molecular pharmaceutics*. 2019;17(2):472-87.
100. Venditto VJ, Szoka Jr FC. Cancer nanomedicines: so many papers and so few drugs! *Advanced drug delivery reviews*. 2013;65(1):80-8.
101. Frank MM, Fries LF. The role of complement in inflammation and phagocytosis. *Immunology today*. 1991;12(9):322-6.

102. Weber C, Voigt M, Simon J, Danner A-K, Frey H, Mailänder V, Helm M, Morsbach S, Landfester K. Functionalization of liposomes with hydrophilic polymers results in macrophage uptake independent of the protein corona. *Biomacromolecules*. 2019;20(8):2989-99.
103. Antimisariis S, Marazioti A, Kannavou M, Natsaridis E, Gkartziou F, Kogkos G, Mourtas S. Overcoming barriers by local drug delivery with liposomes. *Advanced Drug Delivery Reviews*. 2021.
104. Li J, Tan T, Zhao L, Liu M, You Y, Zeng Y, Chen D, Xie T, Zhang L, Fu C. Recent advancements in liposome-targeting strategies for the treatment of gliomas: A systematic review. *ACS Applied Bio Materials*. 2020;3(9):5500-28.
105. Zylberberg C, Matosevic S. Pharmaceutical liposomal drug delivery: a review of new delivery systems and a look at the regulatory landscape. *Drug delivery*. 2016;23(9):3319-29.
106. Torchilin VP, Omelyanenko VG, Papisov MI, Bogdanov Jr AA, Trubetskoy VS, Herron JN, Gentry CA. Poly (ethylene glycol) on the liposome surface: on the mechanism of polymer-coated liposome longevity. *Biochimica et Biophysica Acta (BBA)-Biomembranes*. 1994;1195(1):11-20.
107. Lasic D, Martin F, Gabizon A, Huang S, Papahadjopoulos D. Sterically stabilized liposomes: a hypothesis on the molecular origin of the extended circulation times. *Biochimica et Biophysica Acta (BBA)-Biomembranes*. 1991;1070(1):187-92.
108. Moghimi SM, Szebeni J. Stealth liposomes and long circulating nanoparticles: critical issues in pharmacokinetics, opsonization and protein-binding properties. *Progress in lipid research*. 2003;42(6):463-78.
109. Owens III DE, Peppas NA. Opsonization, biodistribution, and pharmacokinetics of polymeric nanoparticles. *International journal of pharmaceutics*. 2006;307(1):93-102.
110. Palchetti S, Colapicchioni V, Digiacomo L, Caracciolo G, Pozzi D, Capriotti AL, La Barbera G, Laganà A. The protein corona of circulating PEGylated liposomes. *Biochimica et Biophysica Acta (BBA)-Biomembranes*. 2016;1858(2):189-96.
111. Tavakoli S, Kari OK, Turunen T, Lajunen T, Schmitt M, Lehtinen J, Tasaka F, Parkkila P, Ndika J, Viitala T. Diffusion and Protein Corona Formation of Lipid-Based Nanoparticles in the Vitreous Humor: Profiling and Pharmacokinetic Considerations. *Molecular pharmaceutics*. 2020;18(2):699-713.
112. Stepniewski M, Pasenkiewicz-Gierula M, Róg T, Danne R, Orlowski A, Karttunen M, Urtti A, Yliperttula M, Vuorimaa E, Bunker A. Study of PEGylated lipid layers as a model for PEGylated liposome surfaces: molecular dynamics simulation and Langmuir monolayer studies. *Langmuir*. 2011;27(12):7788-98.
113. Magarkar A, Karakas E, Stepniewski M, Róg T, Bunker A. Molecular dynamics simulation of PEGylated bilayer interacting with salt ions: a model of the liposome surface in the bloodstream. *The Journal of Physical Chemistry B*. 2012;116(14):4212-9.
114. Magarkar A, Rog T, Bunker A. Molecular dynamics simulation of PEGylated membranes with cholesterol: building toward the DOXIL formulation. *The Journal of Physical Chemistry C*. 2014;118(28):15541-9.
115. Lehtinen J, Magarkar A, Stepniewski M, Hakola S, Bergman M, Róg T, Yliperttula M, Urtti A, Bunker A. Analysis of cause of failure of new targeting peptide in PEGylated liposome: molecular modeling as rational design tool for nanomedicine. *European journal of pharmaceutical sciences*. 2012;46(3):121-30.
116. Dzieciuch M, Rissanen S, Szydłowska N, Bunker A, Kumorek M, Jamroz D, Vattulainen I, Nowakowska M, Rog T, Kepczynski M. PEGylated

- liposomes as carriers of hydrophobic porphyrins. *The Journal of Physical Chemistry B*. 2015;119(22):6646-57.
117. Dutta P, Pramanik D, Singh JK. Phase Behavior of Pure PSLC and PEGylated Multicomponent Lipid and Their Interaction with Paclitaxel: An All-Atom MD Study. *Langmuir*. 2021;37(34):10259-71.
118. Dams ET, Laverman P, Oyen WJ, Storm G, Scherphof GL, Van der Meer JW, Corstens FH, Boerman OC. Accelerated blood clearance and altered biodistribution of repeated injections of sterically stabilized liposomes. *Journal of Pharmacology and Experimental Therapeutics*. 2000;292(3):1071-9.
119. Laverman P, Carstens MG, Boerman OC, Dams ETM, Oyen WJ, van Rooijen N, Corstens FH, Storm G. Factors affecting the accelerated blood clearance of polyethylene glycol-liposomes upon repeated injection. *Journal of Pharmacology and Experimental Therapeutics*. 2001;298(2):607-12.
120. Ishida T, Atobe K, Wang X, Kiwada H. Accelerated blood clearance of PEGylated liposomes upon repeated injections: effect of doxorubicin-encapsulation and high-dose first injection. *Journal of controlled release*. 2006;115(3):251-8.
121. Vanić Z, Barnert S, Süß R, Schubert R. Fusogenic activity of PEGylated pH-sensitive liposomes. *Journal of liposome research*. 2012;22(2):148-57.
122. Slepishkin VA, Simões S, Dazin P, Newman MS, Guo LS, de Lima MCP, Düzgüneş N. Sterically stabilized pH-sensitive liposomes, intracellular delivery of aqueous contents and prolonged circulation in vivo. *Journal of Biological Chemistry*. 1997;272(4):2382-8.
123. Chen D, Liu W, Shen Y, Mu H, Zhang Y, Liang R, Wang A, Sun K, Fu F. Effects of a novel pH-sensitive liposome with cleavable esterase-catalyzed and pH-responsive double smart mPEG lipid derivative on ABC phenomenon. *International journal of nanomedicine*. 2011;6:2053.
124. Simões S, Moreira JN, Fonseca C, Düzgüneş N, de Lima MCP. On the formulation of pH-sensitive liposomes with long circulation times. *Advanced drug delivery reviews*. 2004;56(7):947-65.
125. Ferreira DdS, Lopes SCdA, Franco MS, Oliveira MC. pH-sensitive liposomes for drug delivery in cancer treatment. *Therapeutic delivery*. 2013;4(9):1099-123.
126. Fan Y, Chen C, Huang Y, Zhang F, Lin G. Study of the pH-sensitive mechanism of tumor-targeting liposomes. *Colloids and Surfaces B: Biointerfaces*. 2017;151:19-25.
127. Aghdam MA, Bagheri R, Mosafer J, Baradaran B, Hashemzadei M, Baghbanzadeh A, de la Guardia M, Mokhtarzadeh A. Recent advances on thermosensitive and pH-sensitive liposomes employed in controlled release. *Journal of Controlled Release*. 2019;315:1-22.
128. Torchilin VP, Zhou F, Huang L. pH-sensitive liposomes. *Journal of liposome research*. 1993;3(2):201-55.
129. Ellens H, Bentz J, Szoka FC. pH-induced destabilization of phosphatidylethanolamine-containing liposomes: role of bilayer contact. *Biochemistry*. 1984;23(7):1532-8.
130. Kulig W, Jurkiewicz P, Olżyńska A, Tynkkyne J, Javanainen M, Manna M, Rog T, Hof M, Vattulainen I, Jungwirth P. Experimental determination and computational interpretation of biophysical properties of lipid bilayers enriched by cholesteryl hemisuccinate. *Biochimica et Biophysica Acta (BBA)-Biomembranes*. 2015;1848(2):422-32.
131. Hafez IM, Cullis PR. Cholesteryl hemisuccinate exhibits pH sensitive polymorphic phase behavior. *Biochimica et Biophysica Acta (BBA)-Biomembranes*. 2000;1463(1):107-14.

132. Mahmoudzadeh M, Magarkar A, Koivuniemi A, Rog T, Bunker A. Mechanistic insight into how PEGylation reduces the efficacy of pH-sensitive liposomes from molecular dynamics simulations. *Molecular Pharmaceutics*. 2021;18(7):2612-21.
133. Hafez IM, Cullis PR. Roles of lipid polymorphism in intracellular delivery. *Advanced drug delivery reviews*. 2001;47(2-3):139-48.
134. Tate MW, Gruner SM. Temperature dependence of the structural dimensions of the inverted hexagonal (HII) phase of phosphatidylethanolamine-containing membranes. *Biochemistry*. 1989;28(10):4245-53.
135. Turner DC, Gruner SM. X-ray diffraction reconstruction of the inverted hexagonal (HII) phase in lipid-water systems. *Biochemistry*. 1992;31(5):1340-55.
136. Harper PE, Mannock DA, Lewis RN, McElhaney RN, Gruner SM. X-ray diffraction structures of some phosphatidylethanolamine lamellar and inverted hexagonal phases. *Biophysical Journal*. 2001;81(5):2693-706.
137. Rand R, Fuller N. Structural dimensions and their changes in a reentrant hexagonal-lamellar transition of phospholipids. *Biophysical journal*. 1994;66(6):2127-38.
138. Rappolt M, Hickel A, Bringezu F, Lohner K. Mechanism of the lamellar/inverse hexagonal phase transition examined by high resolution x-ray diffraction. *Biophysical journal*. 2003;84(5):3111-22.
139. Ramezani M, Schmidt M, Bashe B, Pruijm J, Link M, Cullis P, Harper P, Thewalt J, Tieleman D. Structural Properties of Inverted Hexagonal Phase: A Hybrid Computational and Experimental Approach. *Langmuir*. 2020;36(24):6668-80.
140. Ramezani M, Leung S, Delgado-Magnero K, Bashe B, Thewalt J, Tieleman D. Computational and experimental approaches for investigating nanoparticle-based drug delivery systems. *Biochimica et Biophysica Acta (BBA)-Biomembranes*. 2016;1858(7):1688-709.
141. Leach AR. *Molecular modelling: principles and applications*: Pearson education; 2001.
142. Bunker A, Róg T. Mechanistic understanding from molecular dynamics simulation in pharmaceutical research 1: drug delivery. *Frontiers in Molecular Biosciences*. 2020:371.
143. Hospital A, Goñi JR, Orozco M, Gelpí JL. Molecular dynamics simulations: advances and applications. *Advances and applications in bioinformatics and chemistry: AABC*. 2015;8:37.
144. Kollman PA, Massova I, Reyes C, Kuhn B, Huo S, Chong L, Lee M, Lee T, Duan Y, Wang W. Calculating structures and free energies of complex molecules: combining molecular mechanics and continuum models. *Accounts of chemical research*. 2000;33(12):889-97.
145. Kästner J. *Umbrella sampling*. *Wiley Interdisciplinary Reviews: Computational Molecular Science*. 2011;1(6):932-42.
146. van Gunsteren WF, Dolenc J, Mark AE. Molecular simulation as an aid to experimentalists. *Current opinion in structural biology*. 2008;18(2):149-53.
147. Bouzo BnL, Calvelo M, Martín-Pastor M, García-Fandiño R, de la Fuente M. In Vitro–In Silico Modeling Approach to Rationally Designed Simple and Versatile Drug Delivery Systems. *The Journal of Physical Chemistry B*. 2020;124(28):5788-800.
148. Hess B, Kutzner C, Van Der Spoel D, Lindahl E. GROMACS 4: algorithms for highly efficient, load-balanced, and scalable molecular simulation. *Journal of chemical theory and computation*. 2008;4(3):435-47.

149. Phillips JC, Braun R, Wang W, Gumbart J, Tajkhorshid E, Villa E, Chipot C, Skeel RD, Kale L, Schulten K. Scalable molecular dynamics with NAMD. *Journal of computational chemistry*. 2005;26(16):1781-802.
150. Brooks BR, Brooks III CL, Mackerell Jr AD, Nilsson L, Petrella RJ, Roux B, Won Y, Archontis G, Bartels C, Boresch S. CHARMM: the biomolecular simulation program. *Journal of computational chemistry*. 2009;30(10):1545-614.
151. Case DA, Cheatham III TE, Darden T, Gohlke H, Luo R, Merz Jr KM, Onufriev A, Simmerling C, Wang B, Woods RJ. The Amber biomolecular simulation programs. *Journal of computational chemistry*. 2005;26(16):1668-88.
152. Abraham M, Van Der Spoel D, Lindahl E, Hess B, and the GROMACS development team. GROMACS user manual version 5.0. 4, GROMACS User Manual version 5.0.4, www.gromacs.org. 2014.
153. Ryckaert J-P, Ciccotti G, Berendsen HJ. Numerical integration of the cartesian equations of motion of a system with constraints: molecular dynamics of n-alkanes. *Journal of computational physics*. 1977;23(3):327-41.
154. Hess B, Bekker H, Berendsen HJ, Fraaije JG. LINCS: a linear constraint solver for molecular simulations. *Journal of computational chemistry*. 1997;18(12):1463-72.
155. Hünenberger PH. Thermostat algorithms for molecular dynamics simulations. *Advanced computer simulation*: Springer; 2005. p. 105-49.
156. Shuichi N. Constant temperature molecular dynamics methods. *Progress of Theoretical Physics Supplement*. 1991;103:1-46.
157. Basconi JE, Shirts MR. Effects of temperature control algorithms on transport properties and kinetics in molecular dynamics simulations. *Journal of chemical theory and computation*. 2013;9(7):2887-99.
158. Fuzo CA, Degève L. Effect of the thermostat in the molecular dynamics simulation on the folding of the model protein chignolin. *Journal of molecular modeling*. 2012;18(6):2785-94.
159. Bussi G, Donadio D, Parrinello M. Canonical sampling through velocity rescaling. *The Journal of chemical physics*. 2007;126(1):014101.
160. Berendsen HJ, Postma Jv, Van Gunsteren WF, DiNola A, Haak JR. Molecular dynamics with coupling to an external bath. *The Journal of chemical physics*. 1984;81(8):3684-90.
161. Parrinello M, Rahman A. Polymorphic transitions in single crystals: A new molecular dynamics method. *Journal of Applied physics*. 1981;52(12):7182-90.
162. Levitt M, Hirshberg M, Sharon R, Daggett V. Potential energy function and parameters for simulations of the molecular dynamics of proteins and nucleic acids in solution. *Computer physics communications*. 1995;91(1-3):215-31.
163. Haddish-Berhane N, Rickus JL, Haghighi K. The role of multiscale computational approaches for rational design of conventional and nanoparticle oral drug delivery systems. *International journal of nanomedicine*. 2007;2(3):315.
164. Schlick T. *Molecular modeling and simulation: an interdisciplinary guide*: Springer; 2002.
165. Jorgensen WL, Tirado-Rives J. The OPLS [optimized potentials for liquid simulations] potential functions for proteins, energy minimizations for crystals of cyclic peptides and crambin. *Journal of the American Chemical Society*. 1988;110(6):1657-66.
166. Wang J, Wolf RM, Caldwell JW, Kollman PA, Case DA. Development and testing of a general amber force field. *Journal of computational chemistry*. 2004;25(9):1157-74.

167. Huang J, MacKerell Jr AD. CHARMM36 all-atom additive protein force field: Validation based on comparison to NMR data. *Journal of computational chemistry*. 2013;34(25):2135-45.
168. Yao Z, Wang J-S, Liu G-R, Cheng M. Improved neighbor list algorithm in molecular simulations using cell decomposition and data sorting method. *Computer physics communications*. 2004;161(1-2):27-35.
169. Patra M, Karttunen M, Hyvönen MT, Falck E, Lindqvist P, Vattulainen I. Molecular dynamics simulations of lipid bilayers: major artifacts due to truncating electrostatic interactions. *Biophysical journal*. 2003;84(6):3636-45.
170. Guo XD, Zhang LJ, Qian Y. Systematic multiscale method for studying the structure–performance relationship of drug-delivery systems. *Industrial & engineering chemistry research*. 2012;51(12):4719-30.
171. Ma Y-q. Insights into the endosomal escape mechanism via investigation of dendrimer–membrane interactions. *Soft Matter*. 2012;8(23):6378-84.
172. Vácha R, Martinez-Veracoechea FJ, Frenkel D. Intracellular release of endocytosed nanoparticles upon a change of ligand–receptor interaction. *ACS nano*. 2012;6(12):10598-605.
173. Man VH, Li MS, Derreumaux P, Wang J, Nguyen PH. Molecular Mechanism of Ultrasound-Induced Structural Defects in Liposomes: A Nonequilibrium Molecular Dynamics Simulation Study. *Langmuir*. 2021.
174. Wu X, Dai X, Liao Y, Sheng M, Shi X. Investigation on drug entrapment location in liposomes and transfersomes based on molecular dynamics simulation. *Journal of Molecular Modeling*. 2021;27(4):1-10.
175. Lai MZ, Vail WJ, Szoka FC. Acid-and calcium-induced structural changes in phosphatidylethanolamine membranes stabilized by cholesteryl hemisuccinate. *Biochemistry*. 1985;24(7):1654-61.
176. Klasczyk B, Panzner S, Lipowsky R, Knecht V. Fusion-relevant changes in lipid shape of hydrated cholesterol hemisuccinate induced by pH and counterion species. *The Journal of Physical Chemistry B*. 2010;114(46):14941-6.
177. Cullis PR, Hope MJ, Tilcock CP. Lipid polymorphism and the roles of lipids in membranes. *Chemistry and physics of lipids*. 1986;40(2-4):127-44.
178. McIntosh TJ, Simon SA. Adhesion between phosphatidylethanolamine bilayers. *Langmuir*. 1996;12(6):1622-30.
179. Tirosh O, Barenholz Y, Katzhendler J, Prieve A. Hydration of polyethylene glycol-grafted liposomes. *Biophysical journal*. 1998;74(3):1371-9.
180. Holland JW, Cullis PR, Madden TD. Poly (ethylene glycol)–lipid conjugates promote bilayer formation in mixtures of non-bilayer-forming lipids. *Biochemistry*. 1996;35(8):2610-7.
181. Bentz J, Ellens H, Szoka FC. Destabilization of phosphatidylethanolamine-containing liposomes: hexagonal phase and asymmetric membranes. *Biochemistry*. 1987;26(8):2105-16.
182. Mahmoudzadeh M, Fassihi A, Emami J, Davies NM, Dorkoosh F. Physicochemical, pharmaceutical and biological approaches toward designing optimized and efficient hydrophobically modified chitosan-based polymeric micelles as a nanocarrier system for targeted delivery of anticancer drugs. *Journal of drug targeting*. 2013;21(8):693-709.

